Diffraction of light by sound in solids

Yu. V. Gulyaev, V. V. Proklov, and G. N. Shkerdin

Institute of Radio Engineering and Electronics, USSR Academy of Sciences
Usp. Fiz. Nauk 124, 61–111 (January 1978)

Papers on acousto-optical phenomena in solids and their most important applications to research in solid state physics and to modern technology are surveyed. The theory of the diffraction of electromagnetic waves by sound in isotropic and anisotropic solids is discussed. In addition to such "classical" special cases of diffraction as Bragg and Raman-Nath diffraction, we also consider some cases of the diffraction of light by sound in which the reflection of light at the faces of the crystal and modulation of the light by the sound wave have an important effect on the nature of the acousto-optical interaction. The contribution of the electron density wave accompanying a sound wave in piezoactive semiconductors is considered and features of this acousto-optical interaction mechanism are discussed. The quantum theory of the diffraction of light by sound is examined. Microscopic expressions for the photoelasticity constants are obtained and the resonance characteristics of these constants at photon energies close to the width of the forbidden gap in the crystal are investigated. In the experimental part of the paper we review various methods of investigating the diffraction of light by sound in solids and present the basic results in this field together with examples of the use of acousto-optical methods in various areas of solid state physics. In the concluding section we examine some important applications of the diffraction of light by sound to modern optical and electronic systems.

PACS numbers: 43.35.Sx, 78.20.Hp

CONTENTS

INTRODUCTION

The interaction of light with acoustic lattice vibrations of crystals was first discussed theoretically by Brillouin[1] and Mandel'shtam.[2] The first experimental observations of this interaction, by Debye and Sears[3] and by Lucas and Biquard[4] in 1932, pertained to an important special case—the diffraction of light by coherent sound of external origin. Later many studies, both theoretical and experimental, were devoted to these phenomena, and interaction constants, the characteristics of the vibrational spectra of crystals, fluctuation phenomena, and other physical properties of solids and liquids were investigated.

The possibilities of these methods have considerably expanded in recent years because of the development of powerful coherent light sources—lasers. Then with the appearance of powerful sources of coherent sound with frequencies of tens of megahertz and higher the phenomena accompanying the interaction of light and sound also acquired great practical importance, both as means for effectively controlling (deviating, scanning, modulating, etc.) luminous radiation, and as optical methods for processing data expressed as acoustic signals. These phenomena involving both coherent light and coherent sound have come to be called acousto-optical effects, and the study of these phenomena, acousto-optics.

By now there are a number of review articles in the literature in which physical phenomena associated with the scattering of light by thermal fluctuations of crystal lattices[5] as well as acousto-optical phenomena and their applications[6–9] are discussed. Recently, however, in connection with the rapid development of acousto-electronics, a number of new aspects of these phenomena have come to light, which are associated, in particular, with peculiarities of the acousto-optical interaction in conducting crystals, with the amplification of acoustic fluctuations associated with the supersonic drift of electrons, with the appearance of specific acousto-electronic nonlinear effects, etc. Study of these phenomena will make it possible to extend the range of frequencies of electromagnetic radiation that can be controlled by acousto-optical methods considerably beyond the limits of the traditional "optical" range in accordance with the needs of modern technology.

In this review we attempt to describe the interaction of coherent electromagnetic waves with coherent acoustic waves in dielectric and conducting solids from a unified point of view and to point out some important applications of these phenomena to physical research on solids and to modern technology.

1. THEORY OF THE DIFFRACTION OF ELECTROMAGNETIC WAVES BY SOUND IN SOLIDS

In order to construct a completely general theory of the diffraction of electromagnetic waves by sound waves

 0038-5670/78/2101-0029$01.10

in solids one would have to treat the interaction between the two kinds of waves by quantum mechanics. By taking all the mechanisms for this interaction rigorously into account one could make an exact calculation of the diffraction efficiency, which will be determined by the characteristics of the electromagnetic and sound waves, as well as by those of the solid in which the interaction between the waves takes place. However, such a general calculation of the diffraction of electromagnetic waves by sound would be extremely complicated.

The most widely used approach to the approximate solution of this problem is to treat the interaction of the electromagnetic and sound waves phenomenologically, introducing the photoelasticity constants that characterize the change in the dielectric constant of the specimen brought about by the propagation of sound. Such an approach is valid if the frequency of the sound is low compared with the frequency of the electromagnetic wave and with the reciprocal times characteristic of the processes that determine the dielectric constant of the material. Then by using specific models of the mechanisms for the interaction of the electromagnetic and sound waves one can derive specific expressions for the photoelasticity constants thus introduced.

In the first part of this section we use the phenomenological approach to the construction of a theory of the diffraction of electromagnetic waves by sound in solids. However, we shall explicitly take into account the contribution to the diffraction made by the conduction electrons, which is associated with the generation of electron waves that accompany the sound wave. It is assumed that the electromagnetic and acoustic waves, as well as their interaction with the conduction electrons, can be treated classically, i.e., it is assumed that the following two groups of inequalities are satisfied: $\lambda_l \ll l$, Λ, λ, where λ_l is the de Broglie wavelength of the electron, l is the electron mean free path, and λ and Λ are the wavelengths of light and sound (in this case the electrons can be treated as localized particles); and $\hbar\omega \ll E_g$, ε_{av}, where ω is the frequency of light, E_g is the width of the forbidden gap in the crystal, and ε_{av} is the average energy of the conduction electrons. In this case the contribution of the conduction electrons to the (in general complex) dielectric constant of the specimen can be described by an expression involving the effective mass of the electrons.[10,11] When the absorption of the light can be neglected and the main contribution to the diffraction comes from the modulation of the real part of the dielectric constant by the sound wave, the inequality $\hbar\omega \ll E_g$ still remains essential.

In the second part of this section we construct a quantum mechanical theory of the diffraction of light by sound in conducting crystals for cases in which the above inequalities may not be satisfied. We shall examine the most frequently encountered case in which the main contribution to the polarizability of the crystal comes from the electronic polarizability and expressions for the previously introduced photoelasticity constants can be derived on the basis of a microscopic calculation. To keep the calculations simple we shall assume that the interaction of the electromagnetic and acoustic waves with the conduction electrons of the crystal can be treated in the collisionless regime, i.e., that it may be assumed that $ql, \omega\tau \gg 1$, where q is the propagation vector of the sound and τ is the mean relaxation time of the conduction-electron momentum.

a) Classical theory of the diffraction of electromagnetic waves by sound in solids

1) *Method of calculation and the mean approximations.* When electromagnetic and acoustic waves propagate in a solid, their amplitudes, because of their interaction with one another, will be functions of the coordinates within the specimen. To calculate the amplitudes of these waves one must simultaneously solve Maxwell's equations, the equation for the propagation of the sound wave, and Boltzmann's kinetic equation for the electric current density due to the action of the fields of the two waves on the free charge carriers.

This set of equations has the form[12,13]:

$$\operatorname{rot}\mathbf{E} = -\frac{1}{c}\frac{\partial \mathbf{H}}{\partial t}, \qquad (1.1)$$

$$\operatorname{rot}\mathbf{H} = \frac{1}{c}\frac{\partial \mathbf{D}}{\partial t} + \frac{4\pi}{c}\mathbf{j}, \qquad (1.2)$$

$$\operatorname{div}\mathbf{D} = 4\pi(n-n_0)e, \qquad (1.3)$$

$$\rho\frac{\partial^2 U_i}{\partial t^2} = \frac{\partial \sigma_{ik}}{\partial r_k}, \qquad (1.4)$$

$$\mathbf{j} = \frac{e}{4\pi^3}\int \mathbf{v}f(\mathbf{r}, \mathbf{v}, t)\, d^3\mathbf{k}, \qquad (1.5)$$

$$\frac{\partial f}{\partial t} + \mathbf{v}\frac{\partial f}{\partial \mathbf{r}} + \left[e\left(\mathbf{E} + \frac{[\mathbf{vH}]}{c}\right) - \Lambda_{ik}\frac{\partial U_{ik}}{\partial \mathbf{r}}\right]\frac{\partial f}{\partial \mathbf{p}} = I_{\mathrm{coll}}, \qquad (1.6)$$

where

$$D_i = \varepsilon_{ik}E_k - 4\pi\beta_{i,kl}U_{kl}, \qquad (1.7)$$

$$\sigma_{ik} = c_{ikmn}U_{mn} + \beta_{l,ik}E_l + \Lambda_{ik}n + \frac{\varepsilon^0_{ml}\varepsilon^0_{nj}P_{ljik}E_mE_n}{8\pi}, \qquad (1.8)$$

$$\varepsilon_{ik} = \varepsilon^0_{ik} - \varepsilon^0_{il}\varepsilon^0_{km}P_{lmnj}U_{nj}. \qquad (1.9)$$

In Eqs. (1.1)–(1.9) $\mathbf{E}$ and $\mathbf{H}$ represent the electric and magnetic field strengths in the electromagnetic wave within the specimen (which is assumed to be nonmagnetic); n and n_0 are the local and equilibrium values of the free-carrier density, respectively, while $\mathbf{j}$ is the electric current density; $\mathbf{U}$ is the mechanical displacement within the sound wave, while U_{ik} is the deformation tensor of the crystal; the components of the tensors $\beta_{i,kl}$ and Λ_{ik} are the piezomoduli and the deformation potentials of the crystal, respectively; P_{ljik} is the elasto-optical tensor; ε^0_{ik} is the lattice dielectric permittivity in the absence of sound; I_{coll} is the collision integral for collisions of the charge carriers with the scatterers; and f is the distribution function for the free charge carriers.

In the subsequent calculations we assume that the intensity of the sound wave is low enough (and that of the electromagnetic wave high enough) that the change in the intensity of the sound resulting from diffraction may be neglected and induced scattering of light[1)] need not be

[1)]Induced scattering of light by sound is of considerable interest, but it requires special treatment—see, e.g., Ref. 5 (a review article), as well as Refs. 7 and 16–19.

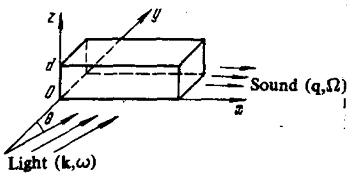

FIG. 1.

considered. In this case the calculation of the fields of the electromagnetic wave in the specimen is much simpler—it reduces to the solution of Maxwell's equations under the boundary conditions that the tangential components of **E** and **H** be continuous at the boundaries of the specimen.

This method of calculation, based on the solution of Maxwell's equations, is the most convenient for calculating the fields of an electromagnetic wave in the near zone when diffraction effects due to the finite aperture of the incident electromagnetic radiation are small and can be neglected.

To solve the problem one can also use the method of integral equations, which is developed in Refs. 15 and 20 for the case of dielectrics; in this case the calculation is simplest in the distant-field approximation.

To simplify the calculations we shall limit ourselves henceforth to the following geometric situation, which usually obtains in experiments on diffraction of light by sound (Fig. 1).

The sound wave with propagation vector **q** and frequency Ω propagates in the specimen along the x axis, while a plane electromagnetic wave of frequency ω ($\omega \gg \Omega$), whose propagation vector **k** lies in the (x, y) plane and makes an angle θ with the y axis, strikes the face $y=0$ of the specimen, it being assumed that nothing in the specimen depends on the coordinate z. In this case Eqs. (1.1) and (1.2) yield the following equation for the electric field of the electromagnetic wave in the specimen:

$$\left(\frac{\partial^2}{\partial x^2}+\frac{\partial^2}{\partial y^2}\right)E_i-\frac{1}{c^2}\frac{\partial^2}{\partial t^2}(\varepsilon_{ik}E_k)-\frac{\partial}{\partial r_i}(\operatorname{div}\mathbf{E})-\frac{4\pi}{c^2}\frac{\partial j_i}{\partial t}=0, \tag{1.10}$$

where ε_{ik} is given by Eq. (1.9); here **j** is the electric current density induced by the propagating electromagnetic wave and is to be found by solving the kinetic equation.

In what follows we shall use the expression

$$j_i=\sigma_{ik}E_k, \tag{1.11}$$

for **j**, where $\sigma_{ik}=\sigma_{ik}(\omega)$ is the high-frequency conductivity of the specimen.[2)] In the region $\omega\tau_p \gg 1$, which is the most interesting region from the standpoint of acoustooptics, and in the effective mass approximation for the conduction electrons, we have $\sigma_{ik}=(ie^2/\omega)n(m^*_{ik})^{-1}$, where τ_p and $(m^*_{ik})^{-1}$ are the momentum relaxation time and the reciprocal effective mass tensor, respectively, for the conduction electrons.

For the propagation of a sound wave in a crystal, the quantities ε_{ik} and σ_{ik} can generally be written as follows[3)]:

$$\varepsilon_{ik}(x,y,t)=\sum_{m=-\infty}^{\infty}\varepsilon^m_{ik}(x,y)\,e^{im(qx-\Omega t)}, \tag{1.12}$$

$$\sigma_{ik}(x,y,t)=\sum_{m=-\infty}^{\infty}\sigma^m_{ik}(x,y)\,e^{im(qx-\Omega t)}, \tag{1.13}$$

where $\Omega=2\pi/T$ and $q=2\pi/\Lambda$, where T and Λ are the period and wavelength of the sound wave. The x and y dependences of ε^m_{ik} and σ^m_{ik} arise, for example, in connection with the propagation of acoustic surface waves (ASW) with allowance for their absorption in the crystal (it is assumed that σ^m_{ik} and ε^m_{ik} vary much less rapidly with x than e^{iqx}).

Now we write the solution of Eq. (1.10) as the series

$$E_i(x,y,t)=\sum_l V_{i,l}(x,y)\exp\{i[(k\sin\theta+lq)x-(\omega+l\Omega)t]\} \tag{1.14}$$

and, substituting (1.11)–(1.14) into (1.10) and equating coefficients of identical exponentials, we obtain the following recurrence set of differential equations for the functions $V_{i,l}$ which is accurate to terms of the order of Ω/ω:

$$\begin{aligned}&\frac{\partial^2 V_{i,l}(x,y)}{\partial x^2}+\frac{\partial^2 V_{i,l}(x,y)}{\partial y^2}+2i(k\sin\theta+lq)\frac{\partial V_{i,l}}{\partial x}-(k\sin\theta+lq)^2V_{i,l}\\&-\left[i(k\sin\theta+lq)\delta_{i,x}+\frac{\partial}{\partial r_i}\right]\left(\frac{\partial V_{y,l}}{\partial y}+\frac{\partial V_{x,l}}{\partial x}+i(k\sin\theta+lq)V_{x,l}\right)\\&=\sum_{m=-\infty}^{\infty}\gamma^m_{ik}V_{k,l-m},\end{aligned} \tag{1.15}$$

where

$$\gamma^m_{ik}=-\frac{\omega^2}{c^2}\left(\varepsilon^m_{ik}+\frac{4\pi i\sigma^m_{ik}}{\omega}\right),\text{and}\ \delta_{i,x}=\begin{cases}1 & \text{for } i=x,\\ 0 & \text{for } i\neq x.\end{cases}$$

By solving Eqs. (1.15) with the exact boundary conditions we can find the unknown fields inside and outside the specimen and thereby solve our problem. In the general case, however, it is extremely difficult to find an exact solution, so investigators in this field generally consider various special cases of the problem for which Eqs. (1.15) and the boundary conditions can be simplified. In the following we consider some characteristic features of the diffraction of electromagnetic waves by sound, and for this purpose we shall simplify the problem; specifically, we shall assume that there is little absorption of sound along the width of the front of the incident electromagnetic wave and shall neglect the possible distortion of the crystal surface resulting from the propagation of the sound wave, i.e., we shall assume that **U** is very nearly parallel to the (z, x) plane.[4)]

[2)]Expression (1.11) is valid in the linear approximation in the amplitude of the electromagnetic wave provided one can neglect terms (which are usually small) of the type $([\mathbf{VH}]/c)\partial f_1/\partial\mathbf{p}$, $\mathbf{v}\cdot\partial f_1/\partial\mathbf{r}$, and $\mathbf{F}\partial f_1/\partial\mathbf{p}$, where **F** is the force exerted by the sound wave on the conduction electrons and f_1 is the electron distribution function in the high frequency field of the light wave.

[3)]The use of these expressions in Eq. (1.10) is valid if the freqeuncy dependence of the complex dielectric permittivity of the material is smooth enough.

[4)]This effect does not arise in the case of acoustic body waves, when **U** is strictly parallel to the (z, x) plane, but in the case of Rayleigh ASW the distortion of the crystal surface contributes substantially to the diffraction and must be taken into account.[21–23]

2) *Diffraction of electromagnetic waves by sound in isotropic conducting crystals.* Let us assume that the sound intensity is low enough that nonlinear effects in the propagation of the sound wave are virtually absent and that both $|\varepsilon^m_{ik}|$ and $|\sigma^m_{ik}|$ are close to zero for $|m| \geq 2$. In this case Eqs. (1.15) for isotropic conducting crystals, for which $\varepsilon^m_{ik}=\varepsilon_m\delta_{ik}$ and $\sigma^m_{ik}=\sigma_m\delta_{ik}$ (i.e., $\gamma^m_{ik}=\gamma_m\delta_{ik}$), take the form

$$\frac{d^2V_{i,l}(y)}{dy^2}-\left[i(k\sin\theta+lq)\delta_{i,x}+\frac{\partial}{\partial r_i}\right]\left[\frac{dV_{y,l}}{dy}+i(k\sin\theta+lq)V_{x,l}\right]+\delta_l V_{i,l}(y)=\gamma_{+1}V_{i,l-1}+\gamma_{-1}V_{i,l+1}, \tag{1.16}$$

where

$$\delta_l=\frac{\omega^2}{c^2}\varepsilon_0(\omega)-(k\sin\theta+lq)^2, \text{ and } \varepsilon_0(\omega)=\varepsilon_0+\frac{4\pi i\sigma_0}{\omega}.$$

It is evident from Eq. (1.16) that the equations for $V_{z,l}$ and $V_{x,y,l}$ are independent of one another (this is associated with the assumption that the specimen is uniform in the direction of the z axis). Hence if the incident electromagnetic wave is polarized along the z axis, the diffracted wave will also be polarized along the z axis. In the following we shall assume that the electric field vector $\mathbf{E}_0$ of the incident electromagnetic wave is parallel to the z axis.

Here too, however, it is very difficult to obtain a general solution to Eqs. (1.16) that satisfies the exact boundary conditions. Hence we shall discuss several special cases that illustrate the principal characteristic properties of diffraction.

a) Let us assume that the intensities of the diffraction orders fall off rapidly with increasing order number $|l|$. In this case, to solve Eqs. (1.16) we may use the successive approximation method (SAM),[1,6,27,29,30,32] which make it possible, in principle, to calculate the intensities of the diffraction orders as accurately as may be desired without any additional limitations. However, even the expressions for the amplitudes $E^{ref}_{\pm 1}$ and $E^{tr}_{\pm 1}$ of the reflected and transmitted diffraction waves of the lowest orders $l=\pm 1$ obtained by using the exact boundary conditions in the first SAM approximation turn out to be rather cumbersome. Here, therefore, we give the simplest expressions for the E^{tr}_l under the assumption that the functions $\gamma_{\pm 1}(y)$ and the amplitudes of the diffracted waves vary little over a wavelength of light and that reflection of light from the specimen may be neglected. In this case Eqs. (1.16) can be reduced to the following set of first order equations:

$$\frac{dU_l}{dy}+i\beta_l U_l=-\frac{i}{2}\left(\frac{\gamma_{+1}}{\sqrt{\delta_0}}U_{l-1}+\frac{\gamma_{-1}}{\sqrt{\delta_0}}U_{l+1}\right), \tag{1.17}$$

where

$$\beta_l=\frac{\delta_0-\delta_l}{2\sqrt{\delta_0}}=\frac{2kql\sin\theta+l^2q^2}{2\sqrt{\delta_0}}.$$

Here we have written $V_l(y)=U_l(y)\exp(i\sqrt{\delta_0}y)$ and have assumed that $U_l(y)$ varies little over a wavelength of light.

Within the limitations of the SAM, the solution of (1.17) for $l>0$ has the form

$$U_l=-\frac{i}{2\sqrt{\delta_0}}e^{-i\beta_l y}\int_0^y \gamma_{+1}(y')e^{i\beta_l y'}U_{l-1}(y')\,dy', \tag{1.18}$$

and in particular, for $l=+1$ we have

$$U_{+1}=-\frac{iE_0}{2\sqrt{\delta_0}}e^{-i\beta_{+1}y}\int_0^y \gamma_{+1}(y')e^{i\beta_{+1}y'}\,dy'. \tag{1.19}$$

When $\gamma_{+1}(y')=\text{const}$, we have

$$U_{+1}(y)=\frac{\gamma_{+1}E_0}{\delta_{+1}-\delta_0}\left(1-e^{-i\beta_{+1}y}\right)$$

and when the absorption of light is neglected the expression for $|V_{+1}(d)|^2$ takes the form (d is the thickness of the specimen in the y direction)

$$|V_{+1}(d)|^2=\frac{E_0^2|\gamma_{+1}|^2d^2}{4\delta_0^2}\left[\sin^2\left(\frac{\delta_0-\delta_{+1}}{4\sqrt{\delta_0}}d\right)\right]\left(\frac{\delta_0-\delta_{+1}}{4\sqrt{\delta_0}}d\right)^{-2}. \tag{1.20}$$

Equations (1.18)–(1.20) were obtained using this simplified boundary conditions $U_l(y=0)=E_0\delta_{l,0}$, which neglect the reflected series of diffracted beams. Analysis shows that the simplified boundary conditions can be applied when the following two conditions are satisfied:

$$R=\left|\frac{k\cos\theta-\sqrt{\delta_0}}{k\cos\theta+\sqrt{\delta_0}}\right|\ll 1, \text{ and } |\delta_l-\delta_0|\ll|\delta_0|.$$

These conditions permit one to neglect reflection of light in the zeroth and higher diffraction orders. In addition, the second condition, as a rule, makes it possible to pass from Eqs. (1.16) to Eqs. (1.17). When $|\delta_l-\delta_0|\sim|\delta_0|$, one cannot assume that the amplitudes $U_l(y)$ of the diffracted waves are slowly varying functions of y and must take into account the modulation of the reflection coefficient R by the sound wave, which gives rise to diffraction in the reflected light even when $R\ll 1$, and in this case, generally speaking, $|E^{ref}_l|\sim|E^{tr}_l|$.

However, the case in which $|\delta_l-\delta_0|\sim|\delta_0|$ for $l=\pm 1, \pm 2, \ldots$ is, as a rule, uninteresting from the point of view of obtaining efficient diffraction at relatively low sound power because of the lack of spatial synchronism between the zeroth and higher orders of diffraction.[5] For example, spatial synchronism between the zeroth and first orders arises just when $|\delta_{+1}-\delta_0|$ is fairly small, and then, because of the increase in the size of the region in which light and sound interact, considerable diffraction efficiency can be achieved even at low sound power. It is evident from Eq. (1.20) that $|V_{+1}(d)|^2\sim d^2$ when $|(\delta_0-\delta_{+1})d/\sqrt{\delta_0}|\ll 1$, and $|V_{+1}(d)|\sim E_0$ when $d\sim\delta_0/|\gamma_{+1}|$.

Further, let us consider some cases in which the diffraction efficiency in reflection and transmission can be considerable and the SAM is not applicable; moreover, in the next two items b) and c) we shall assume that $R\ll 1$ and $|\delta_l-\delta_0|\ll|\delta_0|$ for the diffraction orders l considered, when Eqs. (1.17) are valid and simplified

[5]Here we have not yet considered the case $|\delta_0|\approx 0$, which may be encountered when $\omega\approx\omega_p$, where ω_p is the plasma frequency of the conduction electrons; in that case the diffraction efficiency may be fairly high because of the modulation of R by the sound. Moreover, when $|\delta_0|\approx 0$ one cannot pass from Eqs. (1.16) to Eqs. (1.17).

boundary conditions can be imposed in solving them.

b) If we neglect the absorption of light, i.e., if we assume that $\mathrm{Im}\delta_0 \simeq 0$ and $\gamma_{+1} = \gamma_{-1}^* = |\gamma_{+1}| e^{i\varphi}$, and if the wavelength of sound is also long enough that a term of the order of $l^2 q^2 U_l$ can be neglected, we can rewrite Eqs. (1.17) in the form

$$\frac{d\Phi_l(y)}{dy} + i\,\frac{k(\sin\theta)lq}{\sqrt{\delta_0}}\,\Phi_l(y) = \frac{|\gamma_{+1}|}{2\sqrt{\delta_0}}\,(\Phi_{l+1} - \Phi_{l-1}), \tag{1.21}$$

where $U_l(y) = \Phi_l(y)\exp(i((\pi/2)+\varphi)l)$.

On solving (1.21) under the assumption that the $\gamma_{\pm 1}$ are independent of y, we obtain the following expression for $V_l(y)$:

$$V_l(y) = E_0 \exp\left\{i\left[\sqrt{\delta_0} - l\,\frac{k(\sin\theta)q}{2\sqrt{\delta_0}}\right]y + il\left(\varphi - \frac{\pi}{2}\right)\right\} \times J_l\left\{\frac{|\gamma_{+1}|y}{\sqrt{\delta_0}}\left[\sin\left(\frac{k\sin\theta\cdot q}{2\sqrt{\delta_0}}\,y\right)\right]\left(\frac{k\sin\theta\cdot q}{2\sqrt{\delta_0}}\,y\right)^{-1}\right\}, \tag{1.22}$$

where J_l is the Bessel function of order l.

It is evident from Eq. (1.22) that efficient diffraction is possible in several orders at once in the case under consideration when $|\gamma_{+1}|\,y/\sqrt{\delta_0} \sim 1$. This diffraction region is called the Raman-Nath region for historical reasons. The principal characteristic of diffraction in this region is, as follows from (1.22), that when $R \ll 1$ the electromagnetic wave on leaving the crystal is purely phase modulated, i.e.,

$$E_{\mathrm{tr}} \sim E_0 \exp\left[i\,\frac{|\gamma_{+1}|d}{\sqrt{\delta_0}}\sin\left(qx - \Omega t + \varphi - \frac{\pi}{2}\right)\right]$$

when $\theta \sim 0$ (Refs. 24–27). To calculate the diffraction in this region one may assume that in the specimen there is a plane phase diffraction grating accompanying the acoustic wave, which does not affect the direction of propagation of light in the specimen.[24,27]

c) Now let us assume that $\sin\theta \approx -q/2k$, i.e., that $\delta_0 \approx \delta_{+1}$ and $q^2 d/|\sqrt{\delta_0}| \gg 1$, so that $|\delta_0 - \delta_{-1}|d/|\sqrt{\delta_0}| \gg 1$. In this case, as is evident, for example, from (1.20), $|E_{+1}^{\mathrm{tr}}| \gg |E_{-1}^{\mathrm{tr}}|$ (analysis shows that in this case the higher order diffracted waves are weak). Thus, in solving (1.17) one need consider only two diffraction orders, the zeroth and the +1-th:

$$\frac{dU_0}{dy} = -\frac{i}{2}\,\frac{\gamma_{-1}}{\sqrt{\delta_0}}\,U_{+1}, \tag{1.23}$$

$$\frac{dU_{+1}}{dy} + i\beta_{+1}U_{+1} = -\frac{i}{2}\,\frac{|\gamma_{+1}|}{\sqrt{\delta_0}}\,U_0. \tag{1.24}$$

For the case $R \ll 1$ when γ_{+1} and γ_{-1}^* are equal and independent of y and $\mathrm{Im}\delta_0 \approx 0$, the expressions for the intensities of the zeroth and +1-th orders in transmission are as follows[26,37]:

$$I_0^{\mathrm{tr}} = I_0 - I_{+1}^{\mathrm{tr}}, \tag{1.25}$$

$$I_{+1}^{\mathrm{tr}} = I_0\left(\frac{v}{2\sigma}\sin\sigma\right)^2, \tag{1.26}$$

where

$$\sigma = \frac{1}{2}\sqrt{v^2 + \frac{Q^2}{4}(1-2\alpha)^2},$$

$$v = \frac{|\gamma_{+1}|d}{\sqrt{\delta_0}}, \quad Q = \frac{q^2 d}{\sqrt{\delta_0}},$$

$$\alpha = -\frac{k}{q}\sin\theta.$$

It is evident from Eqs. (1.25) and (1.26) that when $v \lesssim 1$ and $Q \gg 1$ the quantity I_{+1}^{tr} will depend strongly on the angle of incidence θ and will reach its maximum value at $\sin\theta = -q/2k$, where $I_{+1}^{\mathrm{tr}} = I_0\sin^2(v/2)$ and $I_0^{\mathrm{tr}} = I_0\cos^2(v/2)$; then $I_{-1}^{\mathrm{tr}} \sim ((\sin^2 Q)/Q^2)I_{+1}^{\mathrm{tr}} \ll I_{+1}^{\mathrm{tr}}$.

The diffraction region now under consideration is called the region of Bragg reflection of light by sound. The basic characteristic of diffraction in this region is that only two diffraction orders are significant, for example the zeroth and the +1-th, as discussed above. This is due to the fact that here only one diffraction order is in spatial synchronism with the zeroth order. The diffraction process in the Bragg reflection region can be essentially described by acts of emission or absorption of phonons by photons of the incident electromagnetic wave, and to illustrate these acts one can use vector diagrams representing the energy and momentum conservation laws, which are satisfied in these events of interaction of light with sound. In this region the fact that the diffraction grating induced in the specimen by the sound wave is a bulk grating manifests itself in an essential manner, and here the electromagnetic wave on leaving the crystal is modulated, generally speaking, in both amplitude and phase.

Cases a)–c) discussed above are classical and are the best investigated cases of the diffraction of light by sound. It is evident from Eqs. (1.22) and (1.26) that the basic properties of diffraction are characterized by the parameters v, Q, and α. The parameter v characterizes the extent to which energy is transferred from the zeroth order diffracted wave to the higher orders provided the conditions for spatial synchronism between the zeroth order and those higher order diffracted waves are satisfied. The parameters Q and α characterize the extent to which the conditions for spatial synchronism are satisfied. For Q, $Q|\alpha| \ll 1$ with $v \sim 1$, when the conditions for spatial synchronism can be simultaneously satisfied for several orders and their coupling with the zeroth order is sufficiently effective, several important diffraction orders will manifest themselves; for $Q \gg 1$ with $v \sim 1$ the conditions for spatial synchronism and sufficiently effective interaction will be satisfied only for one diffraction order (namely $l = +1$ or $l = -1$) if $\alpha \approx \pm(1/2)$.

The criteria for various special cases of diffraction have been the subject of a number of studies. Analysis shows that the criterion for diffraction in the Bragg region is $Q \gg \max(1, v)$, while the criterion for the Raman-Nath region is $Q \ll \min(1, 1/v)$.[26,38–40] In the intermediate region where the criteria for Bragg and Raman-Nath diffraction are not satisfied it is very difficult to obtain analytic expressions for the amplitudes of the diffracted waves of various orders and one frequently resorts to numerical methods.[26] A method has been developed by Leroy and others[31,40,41] that enables one to find the amplitudes of the diffracted waves of various orders as series in the parameter Q/v (for $\theta \simeq 0$) which, however, is suitable only if Q is fairly small (from results given in Ref. 40 one can obtain the criteria given above for Raman-Nath diffraction).

In concluding this subsection let us consider the case in which there is substantial diffraction in reflected light.

d) Let us assume that the propagation vector of the sound is sufficiently small so that the terms $(2lkq\cdot\sin\theta + l^2q^2)V_l(y)$ in (1.16) can be neglected. Then Eq. (1.16) simplifies greatly, assuming the form

$$\frac{d^2V_l(y)}{dy^2}+\delta_0V_l(y)=\gamma_{+1}V_{l-1}(y)+\gamma_{-1}V_{l+1}(y). \tag{1.27}$$

According to the technique described in Refs. 20 and 27, one can find a solution to (1.27) that satisfies the exact boundary conditions provided $\gamma_{\pm1}(y)$ varies little in a wavelength of the light.

For simplicity we give here the expressions for E_l^{tr} and E_l^{ref}, assuming that $\gamma_{\pm1}(y)=\text{const}$, that were obtained in Ref. 33:

$$E_l^{ref}=\frac{E_0}{\pi}\left(1-\frac{\delta_{l,0}}{2}\right)\int_0^{2\pi}\frac{dx\,e^{-ilx}[1-\xi(x)\delta_{l,0}]}{1+\xi(x)} \times\left[1-\frac{1-\xi(x)+2\xi(x)\delta_{l,0}}{1+\xi(x)}e^{2i\psi(x)}\right]\left[1-\left(\frac{1-\xi(x)}{1+\xi(x)}\right)^2e^{2i\psi(x)}\right]^{-1} \tag{1.28}$$

and

$$E_l^{tr}=\frac{2E_0}{\pi}\int_0^{2\pi}\frac{dx\,e^{-ilx}\xi(x)}{[1+\xi(x)]^2}\,\frac{e^{i\psi(x)}}{1-\{[1-\xi(x)]/[1+\xi(x)]\}^2e^{2i\psi(x)}}, \tag{1.29}$$

where

$$\xi(x)=\frac{\sqrt{\delta_0-\gamma_{+1}e^{ix}-\gamma_{-1}e^{-ix}}}{k\cos\theta},$$

and

$$\psi(x)=\sqrt{\delta_0-\gamma_{+1}e^{ix}-\gamma_{-1}e^{-ix}}\,d.$$

It is most convenient to discuss expressions (1.28) and (1.29) for two special cases: $|\delta_0|\ll|\gamma_{\pm1}|$ and $|\delta_0|\gg|\gamma_{\pm1}|$.

a) Suppose that $|\delta_0|\gg|\gamma_{\pm1}|$. Then neglecting the x dependence of $\xi(x)$, retaining only on the first term in the expansion of $\psi(x)$ in powers of $\gamma_{\pm1}/\delta_0$, and using the integral representation for the Bessel functions,[36] we can reexpress Eqs. (1.28) and (1.29) as follows:

$$E_l^{ref}=E_0(2-\delta_{l,0})\frac{k\cos\theta-\delta_{l,0}\sqrt{\delta_0}}{k\cos\theta+\sqrt{\delta_0}}e^{i\varkappa l}\left[\delta_{l,0}-\frac{2\sqrt{\delta_0}(R+\delta_{l,0})}{k\cos\theta+\sqrt{\delta_0}}\times\sum_{n=1}^{\infty}R^{2n-2}e^{2in\sqrt{\delta_0}d}J_l(2na)\right], \tag{1.30}$$

and

$$E_l^{tr}=\frac{4E_0k\cos\theta\sqrt{\delta_0}}{(k\cos\theta+\sqrt{\delta_0})^2}e^{i\varkappa l}\sum_{n=1}^{\infty}R^{2n-2}e^{i(2n-1)\sqrt{\delta_0}d}J_l[(2n-1)a], \tag{1.31}$$

where

$$a=\frac{\sqrt{\gamma_{+1}\gamma_{-1}}\,d}{\sqrt{\delta_0}},$$

$$\varkappa=\operatorname{arctg}\frac{\gamma_{+1}+\gamma_{-1}}{i(\gamma_{+1}-\gamma_{-1})}$$

($\varkappa=\varphi-(\pi/2)$ if $\gamma_{+1}=\gamma_{-1}^*=|\gamma_{+1}|e^{i\varphi}$), and $R=(k\cos\theta-\sqrt{\delta_0})/(k\cos\theta+\sqrt{\delta_0})$ is the reflection coefficient for the light.

For the case $|R|\ll1$ expressions (1.31) go over into the corresponding expressions (1.22), where one must put $\theta\simeq0$ (i.e., $l(kq\sin\theta/\sqrt{\delta_0})d\ll1$). If the reflection coefficient is not small there will be substantial diffraction in reflected light on account of reflection from the face $y=d$.

b) Now suppose that $|\delta_0|\ll|\gamma_{+1}|$. Such conditions may be encountered at incident-light frequencies close to those for which $\mathrm{Re}\,\delta\approx0$, and when the light absorption is weak enough (e.g., for $\omega\approx\omega_p$). In this case, if we neglect multiple reflections (assuming that $\mathrm{Im}\sqrt{\delta_0+2|\gamma_{+1}|}\,d\gtrsim1$) we can put Eqs. (1.28) and (1.29) in the form

$$E_l^{ref}=\frac{E_0}{\pi}\left(1-\frac{\delta_{l,0}}{2}\right)e^{il\varphi}\int_0^{2\pi}dx\,\frac{(\cos lx)\,[k\cos\theta-\delta_{l,0}\sqrt{-2|\gamma_{+1}|\cos x}]}{k\cos\theta+\sqrt{-2|\gamma_{+1}|\cos x}}, \tag{1.32}$$

$$E_l^{tr}=\frac{2E_0}{\pi}e^{il\varphi}\int_0^{2\pi}dx\,\frac{(\cos lx)\,k\cos\theta\sqrt{-2|\gamma_{+1}|\cos x}}{(k\cos\theta+\sqrt{-2|\gamma_{+1}|\cos x})^2}e^{i\sqrt{\delta_0-2|\gamma_{+1}|\cos x}\,d}, \tag{1.33}$$

where $\gamma_{+1}=|\gamma_{+1}|e^{i\varphi}$ and $\gamma_{-1}=\gamma_{+1}^*$.

It is evident from Eqs. (1.32) and (1.33) that the intensities of all the reflection orders for $l\neq0$ and those of the transmission orders for all l have maxima at $|\gamma_{+1}|\sim k^2\cos^2\theta$, while the intensity of the zeroth order reflection is minimum at that point. Estimates of the intensities of the transmitted and reflected light in the various diffraction orders near the optimum yield the following values[33,34]: $I_0^{ref}\approx0.24I_0$, $I_{\pm1}^{ref}\approx0.1I_0$, $I_{\pm2}^{ref}\approx0.05I_0$, and $I_l^{ref}(|l|\geqslant3)\sim I_0/al^2$, where $a\sim10$, and $I_l^{tr}\simeq I_0e^{-\alpha_e d}/\pi k\cos\theta$ for $kd\cos\theta\gg1$, $|l|$; here I_0 is the intensity of the incident light and $\alpha_e=2\,\mathrm{Im}\sqrt{\delta_0+2|\gamma_{+1}|}\,d$ is the light absorption coefficient.

The condition for an optimum $|\gamma_{+1}|\sim k^2\cos^2\theta$ means that $\Delta n/n_0\sim(\cos^2\theta)/\varepsilon_0$ and for $\varepsilon_0\gg1$, we have $\Delta n/n_0\ll1$, i.e., the concentration nonlinearity attributable to the propagation of the sound is still inconsiderable. It should be pointed out that for the condition $|\delta_0|\ll|\gamma_{+1}|$ to be satisfied near the optimum it is necessary that the condition $\omega\tau_p\gtrsim\varepsilon_0$ be satisfied when the plasma minimum in reflection is clearly manifest.[35]

The physical effect of the appearance of a diffraction optimum can be explained as follows. The frequency ω_{min} of the plasma minimum in reflection and the maximal frequency ω_1 of the light at which total reflection from the specimen takes place are related as follows to the local electron density: $\omega_p^2\omega_{min}^2=1-(1/\varepsilon_0)$ and $\omega_p^2/\omega_1^2=1-((\sin^2\theta)/\varepsilon_0)$ where $\omega_p^2=4\pi ne^2/m^*\varepsilon_0$. Let us fix the frequency $\omega=\omega_1(n_0)$ of the light in the absence of sound when $n=n_0$. The sound wave modulates the electron density and accordingly modulates the frequencies ω_{min} and ω_1. It is precisely in the region of enhanced electron density that we have $\omega<\omega_1$, i.e., in this region virtually all the incident light will be reflected from the specimen. In the region of reduced electron density, however, we have $\omega>\omega_1$, i.e., here the specimen will be partially transparent to the light. Then if the amplitude of the sound is such that in the region of reduced electron density we have $\omega\simeq\omega_{min}$, (i.e., $(n_0-\Delta n)/n_0\approx(1-(1/\varepsilon_0))/(1-((\sin^2\theta)/\varepsilon_0))$ (for $\varepsilon\gg1$ we have $\Delta n/n_0\approx(\cos^2\theta)/\varepsilon_0$), then in this region there will be virtually no reflection of the light. Thus, when $\Delta n/n_0\simeq(\cos^2\theta)/\varepsilon_0$

there arises an amplitude-phase diffraction grating with very high contrast. As the sound intensity increases further the light again begins to be reflected more strongly in the region of reduced electron density and the contrast of the diffraction grating begins to fall.

As is evident from the calculation results presented above the intensity of the diffraction orders is determined both by the amplitude modulation of the dielectric constant $\Delta\varepsilon$ of the lattice and by the amplitude modulation of the conductivity $\Delta\sigma$ of the specimen resulting from the action of the sound wave.

The ratio of the intensity of the electromagnetic wave diffracted by the variations in the electron density (with an amplitude Δn) to the intensity in the electromagnetic wave diffracted by the variations of the dielectric permittivity of the lattice is given, for the case $\omega\tau_p \gg 1$, by the following expression[37]:

$$\xi = \left| \frac{\omega_p^2}{\omega^2} \frac{\varepsilon_0}{\Delta\varepsilon} \frac{\Delta n}{n_0} \right|^2 = \frac{4\pi\rho\eta\varepsilon_{ac}}{\varepsilon_0^4 p^2} \left(\frac{e}{m^*}\right)^2 \frac{\Omega^2}{\omega^4}, \tag{1.34}$$

where p is the photoelasticity constant, η is the coupling constant for the electromagnetic coupling via the piezopotential, and ε_{ac} is the dielectric permittivity at the acoustic frequency.

For Δn in (1.34) we used an expression derived from the linear theory of sound propagation[42] under the conditions $\Omega\tau_M \ll 1$ and $qr_D \ll 1$ where τ_M and r_D are the Maxwell relaxation time and the Debye screening radius for the conduction electrons in the crystal.

It is evident from Eq. (1.34) that $\xi > 1$ provided $\omega < \omega_0$, where ω_0 is given by

$$\omega_0 = 2\sqrt{\pi}\left(\frac{|e|}{m^*}\right)\sqrt{\frac{\varepsilon_{ac}}{\varepsilon_0 v_s c^2}}\sqrt{\frac{\eta}{M_2}\frac{q}{k}}; \tag{1.35}$$

here $M_2 = \varepsilon_0^3 p^2/\rho v_s^3$ is the acousto-optical quality parameter.

Estimates show that for $q \sim k$ we have $\omega_0 \sim 10^{14}$ sec^{-1} for an n-InSb specimen and $\omega_0 \sim 3\times10^{13}$ sec^{-1} for a CdS specimen. Thus, it is possible by using conductive crystals to increase considerably the efficiency of acousto-optical devices at frequencies $\omega < \omega_0$.

3) *Diffraction of electromagnetic waves by sound in anisotropic conducting crystals*. In this subsection we shall examine some of the characteristic features of the diffraction of light by sound in anisotropic crystals. We shall assume the same geometric situation as in subsection 2) and shall also assume that a transverse sound wave propagates in the specimen with the vector **u** parallel to the z axis, which is also the optical axis of the crystal. Such geometry is frequently encountered in experiments on the diffraction of light by sound in anisotropic crystals and is suitable for bringing out sufficiently clearly the principal features of the phenomena of interest that are due to the anisotropy of the crystal. For crystals of the hexagonal system of class C_{6v} (these include the CdS crystal) the dielectric permittivity tensor of the lattice has the following form in this geometry[14]:

$$\varepsilon_{ik} = \begin{pmatrix} \varepsilon_1^0 & 0 & \Delta\varepsilon \\ 0 & \varepsilon_1^0 & 0 \\ \Delta\varepsilon & 0 & \varepsilon_2^0 \end{pmatrix}, \tag{1.36}$$

where $\Delta\varepsilon = -\varepsilon_1^0\varepsilon_2^0 p_{xzzx} u_{zx}$.

We assume that the tensor σ_{ik} is diagonal, i.e., that $\sigma_{ik} = \sigma(i)\delta_{ik}$; moreover, $\sigma_{xx} = \sigma_{yy}$.

Further, the solution to Eqs. (1.15) will be considered under these geometric conditions, using the method of successive approximations, imposing simplified boundary conditions, and neglecting the nonlinearity in density due to the propagation of the sound (i.e., assuming that $|\varepsilon_{ik}^m|$ and $|\sigma_{ik}^m|$ are close to zero for $|m| \geq 2$).

In this case the equations for $V_{i,\pm1}$ take the form

$$\frac{d^2V_{z,\pm1}}{dy^2} + \delta_2^{\pm1}V_{z,\pm1} = \gamma_{zz}^{\pm1}V_{z,0}, \tag{1.37}$$

$$\frac{d^2V_{x,\pm1}}{dy^2} + \frac{\omega^2}{c^2}\varepsilon_1(\omega)V_{x,\pm1} - i(k\sin\theta \pm q)\frac{dV_{y,\pm1}}{dy} = \gamma_{xz}^{\pm1}V_{z,0}, \tag{1.38}$$

$$-i(k\sin\theta \pm q)\frac{dV_{x,\pm1}}{dy} + \delta_1^{\pm1}V_{y,\pm1} = 0, \tag{1.39}$$

where

$$\delta_{1,2}^{\pm1} = \frac{\omega^2}{c^2}\varepsilon_{1,2}(\omega) - (k\sin\theta \pm q)^2, \quad \varepsilon_{1,2}(\omega) = \varepsilon_{1,2}^0 + i\frac{4\pi\sigma_{1,2}}{\omega},$$

$$\gamma_{zz}^{\pm1} = -\frac{4\pi i\omega\sigma_{zz}^{\pm1}}{c^2}, \quad \gamma_{xz}^{\pm1} = -\frac{\omega^2}{c^2}\varepsilon_{xz}^{\pm1};$$

here the tensors γ_{ik}^{+1} have diagonal components due to the modulation of the conductivity by the sound wave and the two components $\gamma_{zx}^{\pm1} = \gamma_{xz}^{\pm1}$ due to photoelasticity.

The solution of Eqs. (1.37)–(1.39) yields the following expressions for $|E_{z,\pm1}^{tr}|$ and $|E_{x,\pm1}^{tr}|$:

$$|E_{z,\pm1}^{tr}| = \left|\frac{\gamma_{zz}^{\pm1}E_0}{\delta_2^{\pm1} - \delta_2^0}\left(e^{i\sqrt{\delta_2^0}d} - e^{i\sqrt{\delta_2^{\pm1}}d}\right)\right|, \tag{1.40}$$

$$|E_{x,\pm1}^{tr}| = \left|\frac{\gamma_{xz}^{\pm1}E_0\delta_1^{\pm1}}{(\delta_1^{\pm1} - \delta_2^0)k^2\varepsilon_1(\omega)}\left(e^{i\sqrt{\delta_2^0}d} - e^{i\sqrt{\delta_1^{\pm1}}d}\right)\right|, \tag{1.41}$$

where $\delta_2^0 = (\omega^2/c^2)\varepsilon_2(\omega) - k^2\sin^2\theta$ and the $\gamma_{ik}^{\pm1}$ are assumed to be independent of y.

It is evident from Eqs. (1.40) and (1.41) that the conditions for Bragg reflection in, say, the +1-th order can be satisfied for two angles of incidence of light in anisotropic crystals, although not in isotropic ones.

a) When $\delta_1^{+1} = \delta_2^0$, i.e., when

$$\sin\theta_n^1 = -\frac{q}{2k\sqrt{\varepsilon_2(\omega)}}\left[1 + \left(\frac{k}{q}\right)^2(\varepsilon_2(\omega) - \varepsilon_1(\omega))\right]$$

anisotropic Bragg reflection of light from sound can take place with change in the modulus of the propagation vector of light owing to a rotation of the polarization vector of the electric field of the diffracted beam of order $l = +1$ through 90° with respect to $\mathbf{E}_0$.[15,43–45] Then the angle at which the diffracted beam propagates in the specimen is given by

$$\sin\theta_D^1 = \frac{q}{2k\sqrt{\varepsilon_1(\omega)}}\left\{1 - \left(\frac{k}{q}\right)^2[\varepsilon_2(\omega) - \varepsilon_1(\omega)]\right\}$$

(here θ_n^1 and θ_D^1 are the angles of incidence and diffraction, and $k = \omega/c$). It is easy to see that collinear Bragg reflection of light is possible in an anisotropic crystal when $(q_{min}/k)^2 = (\sqrt{\varepsilon_2(\omega)} - \sqrt{\varepsilon_1(\omega)})^2$ (q_{min} is the minimum propagation vector of sound at which Bragg reflection with rotation of $\mathbf{E}_0$ through 90° is possible in the anisotropic crystal[9]).

b) When $\delta_2^{+1} = \delta_2^0$, i.e., when $\sin\theta_i^2 = -q/2k\sqrt{\varepsilon_2(\omega)}$, ordinary isotropic Bragg reflection of light from sound can take place without rotation of the polarization vector of the electric field,[26,28,37] anisotropic Bragg reflection taking place when light is diffracted as a result of photoelasticity, and isotropic Bragg reflection, when diffraction is due to electron waves. Hence by appropriately choosing the angles of incidence θ_i^1 and θ_i^2 we can separately investigate the diffraction of light by elastic lattice vibrations, and by electron waves.[46]

Besides the feature discussed above, an additional diffraction mechanism, associated with a rotation of the crystal as the sound wave is propagated, may be operative in anisotropic crystals.[47] In this case one cannot expand the change in the dielectric permittivity of the crystal associated with the propagation of the sound in a series in the deformation tensor, since there is no deformation in the case of pure rotation, but for a given coordinate system the ε_{ik} may vary for an anisotropic crystal. The expression for $\Delta(\varepsilon_{ik})^{-1}$ for pure rotation has the form[47]:

$$\Delta(\varepsilon_{ik})^{-1} = \tilde{P}_{ik[mn]} R_{mn}, \tag{1.42}$$

where

$$R_{mn} = \frac{1}{2}\left(\frac{\partial u_m}{\partial r_n} - \frac{\partial u_n}{\partial r_m}\right)$$

is an antisymmetric tensor characterizing the rotation of the crystal and $\tilde{P}_{ik[mn]} = (1/2)((\varepsilon_{in})^{-1}\delta_{km} + (\varepsilon_{nk})^{-1}\delta_{im} - (\varepsilon_{im})^{-1}\delta_{kn} - (\varepsilon_{mk})^{-1}\delta_{in})$ is a tensor, antisymmetric in the indices m and n. Thus, the general expression for $\Delta(\varepsilon_{ik})^{-1}$ has the following form: $\Delta(\varepsilon_{ik})^{-1} = P_{iklm} u_{lm} + \tilde{P}_{ik[mn]} R_{mn}$, i.e., in highly anisotropic crystals it is reasonable to expand $\Delta(\varepsilon_{ik})$ not in terms of the u_{ik}, but in terms of the $\partial u_i/\partial r_k$. For certain anisotropic crystals, however, the $\tilde{P}_{ik[mn]}$ are small. For example, for a crystal of the CdS type we have

$$\tilde{P}_{xz[xz]} = \frac{1}{2}\left(\frac{1}{\varepsilon_{zz}} - \frac{1}{\varepsilon_{xx}}\right) \approx \frac{\sqrt{\varepsilon_{xx}} - \sqrt{\varepsilon_{zz}}}{\varepsilon^{3/2}} \sim 10^{-3} \ll P_{xzxz},$$

since $P_{xzxz} \approx 0.025$.

Thus, expression (1.9) in the form in which it is written (as also the expressions for $\Delta\varepsilon_{ik}$ given in Refs. 14 and 27, and elsewhere) are valid only for crystals that are not very highly anisotropic.

b) Quantum theory of the diffraction of electromagnetic waves by ultrasound in solids

In the first part of this section we considered the classical theory of the diffraction of electromagnetic waves by sound in conducting crystals, which is valid for comparatively low frequency acoustic and electromagnetic waves when λ_l is small as compared with l, λ, and Λ, and $\hbar\omega$ is small as compared with E_g and ε_{av}. In this part we shall consider the quantum theory of the diffraction of electromagnetic waves by sound, which is valid even for high frequency acoustic and electromagnetic waves when λ_l may not be small as compared with λ and Λ, and $\hbar\omega$ may not be small as compared with E_g (absorption of light will be neglected in the calculations). Further, the calculations in this part will differ from those in the previous part in that here we shall adopt a definite model for the interaction of the electromagnetic and sound waves: specifically, we shall assume that the main contribution to the polarizability of the crystal comes from electronic polarizability. On the basis of this mechanism for the interaction of sound and electromagnetic waves we shall discuss a microscopic theory of the diffraction of electromagnetic waves by sound.

It is clear that in this case one cannot use the classical kinetic equation to describe the interaction of the electrons with the sound and electromagnetic waves; on the contrary, a quantum approach—say on the basis of the density matrix formalism—is necessary in principle. In our exposition we shall confine ourselves to a method similar to the one used in Ref. 17.

For the collisionless case when $\omega\tau_p$ and ql are both large as compared with unity, which was treated in Ref. 50, the coupled set of equations of motion for the photon and phonon creation and annihilation operators, under the assumption that the perturbation of the electron system by the electromagnetic and sound waves is weak, have the following form:

$$\frac{\partial a_{\mathbf{k}}^{+}}{\partial t} = i\omega_k a_{\mathbf{k}}^{+} + i\gamma^{*} a_{\mathbf{k}_1}^{+} b_{\mathbf{q}}^{+}, \tag{1.43}$$

$$\frac{\partial a_{\mathbf{k}_1}^{+}}{\partial t} = i\omega_{k_1} a_{\mathbf{k}_1}^{+} + i\gamma a_{\mathbf{k}}^{+} b_{\mathbf{q}}, \tag{1.44}$$

$$\frac{\partial b_{\mathbf{q}}^{+}}{\partial t} = i\Omega_q b_{\mathbf{q}}^{+} + i\gamma a_{\mathbf{k}}^{+} a_{\mathbf{k}_1}; \tag{1.45}$$

here $a_{\mathbf{k}}^{+}$ and $a_{\mathbf{k}}$ are the creation and annihilation operators for photons with propagation vector $\mathbf{k}$; $b_{\mathbf{q}}^{+}$ and $b_{\mathbf{q}}$ are the creation and annihilation operators for phonons with propagation vector $\mathbf{q}$, it being assumed that $\mathbf{k} = \mathbf{k}_1 + \mathbf{q}$ and $\omega_k = \omega_{k_1} + \Omega_q$, i.e., we are considering one-phonon processes associated with the absorption or emission of a single phonon,

$$\begin{aligned}
\gamma = \frac{1}{\hbar} \sum_{\mathbf{p}, l_1, l} \Bigg\{ \Bigg[\delta(\mathbf{p}, l; \mathbf{p}+\mathbf{q}, l_1) &+ \sum_{l_2} \Bigg(\frac{\beta(\mathbf{p}, l; \mathbf{p}-\mathbf{k}_1, l_2)\,\beta(\mathbf{p}-\mathbf{q}_1, l_2; \mathbf{p}+\mathbf{k}, l_1)}{\varepsilon_{l_1, \mathbf{p}+\mathbf{q}} - \varepsilon_{l_2, \mathbf{p}-\mathbf{k}_1} - \hbar\omega_k} \\
&+ \frac{\beta(\mathbf{p}, l; \mathbf{p}+\mathbf{k}, l_2)\,\beta(\mathbf{p}+\mathbf{k}, l_2; \mathbf{p}+\mathbf{q}, l_1)}{\varepsilon_{l_1, \mathbf{p}+\mathbf{q}} - \varepsilon_{l_2, \mathbf{p}+\mathbf{k}} + \hbar\omega_{k_1}} \Bigg) \Bigg] \Psi_{ik}\Lambda_{ik}(\mathbf{p}+\mathbf{q}, l_1; \mathbf{p}, l)\, Q_{l, l_1, \mathbf{p}} \\
&- \sum_{l_2} \Bigg(\frac{\Psi_{ik}\Lambda_{ik}(\mathbf{p}+\mathbf{q}, l_1; \mathbf{p}, l)\,\beta(\mathbf{p}, l; \mathbf{p}-\mathbf{k}_1, l_2)\,\beta(\mathbf{p}-\mathbf{k}_1, l_2; \mathbf{p}+\mathbf{q}, l_1)\,(\hat{n}_{l, \mathbf{p}} - \hat{n}_{l_2, \mathbf{p}-\mathbf{k}_1})}{(\varepsilon_{l_1, \mathbf{p}+\mathbf{q}} - \varepsilon_{l_2, \mathbf{p}-\mathbf{k}_1} - \hbar\omega_k)(\varepsilon_{l, \mathbf{p}} - \varepsilon_{l_2, \mathbf{p}-\mathbf{k}_1} - \hbar\omega_{k_1})} \\
&- \frac{\Psi_{ik}\Lambda_{ik}(\mathbf{p}+\mathbf{q}, l_1; \mathbf{p}, l)\,\beta(\mathbf{p}, l; \mathbf{p}+\mathbf{k}, l_2)\,\beta(\mathbf{p}+\mathbf{k}, l_2; \mathbf{p}+\mathbf{q}, l_1)\,(\hat{n}_{l, \mathbf{p}} - \hat{n}_{l_2, \mathbf{p}+\mathbf{k}})}{(\varepsilon_{l_1, \mathbf{p}+\mathbf{q}} - \varepsilon_{l_2, \mathbf{p}+\mathbf{k}} + \hbar\omega_{k_1})(\varepsilon_{l, \mathbf{p}} - \varepsilon_{l_2, \mathbf{p}+\mathbf{k}} + \hbar\omega_k)} \Bigg) \Bigg\},
\end{aligned} \tag{1.46}$$

$$Q_{l, l_1, \mathbf{p}} = \frac{\hat{n}_{l, \mathbf{p}} - \hat{n}_{l_1, \mathbf{p}+\mathbf{q}}}{\varepsilon_{l, \mathbf{p}} - \varepsilon_{l_1, \mathbf{p}+\mathbf{q}} + \hbar\Omega_q + i\alpha}, \tag{1.47}$$

$\varepsilon_{l,\mathbf{p}}$ and $\hat{n}_{l,\mathbf{p}}$ are the single-particle energy and the occupation number operator for an electron in the state with propagation vector $\mathbf{p}$ in the l-th energy band, $\Psi_{ik} = i\sqrt{\hbar/2\rho V\Omega_q}\,\xi_i q_k$, $\delta(\mathbf{p}, l; \mathbf{p}+\mathbf{q}, l_1)$ and $\beta(\mathbf{p}, l; \mathbf{p}-\mathbf{k}_1, l_1)$ are respectively the matrix elements of the operators

$$\frac{(\mathbf{e}_{\mathbf{k}}\mathbf{e}_{\mathbf{k}_1})\, 2\pi\hbar e^2 e^{-i\mathbf{q}\mathbf{r}}}{m_0\varepsilon_0\sqrt{\omega_k\omega_{k_1}}\,V}, \qquad -\frac{e}{m_0}\sqrt{\frac{2\pi\hbar}{\varepsilon_0 V\omega_k}}\, e^{i\mathbf{k}_1\mathbf{r}}\hat{\mathbf{p}}\mathbf{e}_{\mathbf{k}_1}$$

between the corresponding Bloch electron states, $\hat{\mathbf{p}} = (\hbar/i)\partial/\partial\mathbf{r}$, $\Lambda_{ik}(\mathbf{p}, l_1; \mathbf{p}-\mathbf{q}, l_2)$ is the matrix element for the electron-phonon interaction via the deformation potential, $\mathbf{e}_{\mathbf{k}}$ is the polarization vector of a photon with propagation vector $\mathbf{k}$, ξ is the polarization vector of a phonon, ρ and V are the density and volume of the crystal, m_0 is the free electron mass, e is the electron charge, and ε_0 is the dielectric constant of the specimen. In deriving Eqs. (1.43)–(1.45) it was assumed that the electron-phonon interaction takes place via the deformation potential.

As was noted above, a similar approach to the treatment of this problem in dielectrics was employed in Refs. 17 and 51, but in those studies phenomenological photoelasticity constants were used. Microscopic calculations of the scattering of light from acoustic phonons in dielectrics have been carried through under similar approximations in Ref. 52, and analogous calculations for the case of scattering in conducting crystals were made in Ref. 53, where the probability for the absorption (or emission) of a phonon by a photon, which is determined by the parameter $|\gamma|$, was calculated.

It is not difficult to obtain a solution to Eqs. (1.43)–(1.45) under the assumption that one of the average occupation numbers $n_{\mathbf{q}}$, $n_{\mathbf{k}}$, and $n_{\mathbf{k}_1}$ for phonons and photons is considerably larger than the others.[6)] Thus, for example, if we assume that $n_{\mathbf{q}}$ is much greater than $n_{\mathbf{k}}$ or $n_{\mathbf{k}_1}$ we obtain the following expressions for the intensities of the electromagnetic radiation in the zeroth and first diffraction orders (assuming that $n_{\mathbf{k}}(0)=0$ when $t=0$):

$$I_1(t) = I_0(0)\sin^2(\xi t), \tag{1.48}$$

$$I_0(t) = I_0(0)\cos^2(\xi t), \tag{1.49}$$

where $I_0(0)$ is the intensity of the zeroth order (with wave vector $\mathbf{k}_1$) at time $t=0$ and $\xi=|\gamma|\sqrt{n_{\mathbf{q}}}$.

To find the intensity of the electromagnetic wave traversing a specimen containing sound waves in the geometry of Fig. 1 for the case $R \ll 1$ we must set $t=d\varepsilon_0/c\sqrt{\varepsilon_0-\sin^2\theta}$ in Eqs. (1.48) and (1.49) and interpret $I_0(0)$ as the intensity of the light incident on the specimen.

In the classical limit, the expression for γ has the form

$$\gamma=\frac{2\pi e^2}{\varepsilon_0\sqrt{\omega_k\omega_{k_1}}}\Psi_{ik}\left[\Lambda_{ik}e_x^0e_y^1(m_{xy}^*)^{-1}Q+\frac{e_x^0e_y^1}{m_0^2\hbar^2}V\tilde{R}_{xy}^{ik}\right], \tag{1.50}$$

where Λ_{ik} is the tensor whose components are the deformation potentials, e_x^0 and e_y^1 are components of the polarization vectors $\mathbf{e}_{\mathbf{k}}$ and $\mathbf{e}_{\mathbf{k}_1}$, $Q=\sum_{\mathbf{p}}Q_{c,c,\mathbf{p}}$ (c is the index for the conduction band), and $\tilde{R}_{xy}^{ik}$ is a tensor that describes the diffraction of light by sound in dielectrics; it unites all the terms in (1.46) except the first term with $l=l_1=c$ and the terms of the second sum with $l=l_1=c$, $l_2\neq c$. The presence of conduction electrons in conducting crystals somewhat alters the value of $\tilde{R}_{xy}^{ik}$ since the summation in $\tilde{R}_{xy}^{ik}$ is actually taken over the free states in the conduction band.[52,53] It has been shown[50] that in this case one obtains full agreement between the results of quantum and classical calculations based on analogous approximations for the Bragg case (for an isotropic crystal described by Eqs. (1.25) and (1.26) with $\sin\theta=-q/2k$). Here the first term in (1.50) corresponds to the contribution to the diffraction from the electron density wave (in choosing the deformation potential constant one must allow for screening by the free charge carriers). Similarly, the second term in (1.50) corresponds to the contribution to the diffraction from the lattice dielectric permittivity wave induced by photoelasticity (this result follows from the relation[52] $R_{xy}^{ik}=(m_0^2\omega^2\hbar^2\varepsilon_0^2/4\pi e^2)P_{yxik}$).

In the essentially quantum region one must use the more general expression (1.46) for γ. The quantum corrections to γ turn out to be the most important when $\hbar\omega_k\simeq E_g$; then resonance enhancement of γ, to which both valence electrons and conduction electrons can contribute, becomes possible.

For the case in which the scattering of light is due mainly to the valence electrons and under the assumption that the matrix elements in the resonance terms in (1.46) can be treated as independent of $\mathbf{p}$ and that the valence and conduction bands are parabolic and that the reduced effective mass of the electrons in them is μ, the efficiency of the first order diffraction is proportional to the following expression[52,54–56]:

$$\frac{I_1}{I_0}\sim\left|\frac{B}{\hbar\Omega_q}\left[\sqrt{E_g-\hbar\omega_k}\,\mathrm{arctg}\sqrt{\frac{\hbar^2p_m^2}{2\mu(E_g-\hbar\omega_k)}}-\sqrt{E_g-\hbar\omega_{k_1}}\,\mathrm{arctg}\sqrt{\frac{\hbar^2p_m^2}{2\mu(E_g-\hbar\omega_{k_1})}}\right]-1\right|^2, \tag{1.51}$$

where B is determined by the matrix elements and is relatively weakly dependent on the frequency of the light and p_m is the propagation vector at the band edge (it is assumed that k and q are both small compared with p_m).

When the frequency of the light is close enough to $E_g/\hbar$, i.e., when $\hbar\Omega_q<E_g-\hbar\omega_k\ll\hbar^2p_m^2/2\mu$, the first term in expression (1.51) increases rapidly with increasing light frequency and the efficiency of the diffraction due to this term takes the form $I_1/I_0\simeq|B|^2/(E_g-\hbar\omega_k)$. It should be noted that Eq. (1.46), and consequently also Eq. (1.51), is valid when the light is not too strongly absorbed, i.e., when $E_g-\hbar\omega_k>\alpha$ and $E_g-\hbar\omega_{k_1}>\alpha$, where α is the width of the dispersion curve. Calculations for dielectrics made by the authors of Refs. 54–56 on the basis of Loudon's theory[52] show satisfactory agreement between theory and experiment. The behavior of the diffraction efficiency with increasing light frequency can be more complicated than a simple monotonic growth, and indeed, as is evident from (1.51), for a certain value of B the diffraction efficiency can vanish at a certain light frequency $\omega<E_g/\hbar$ (Refs. 54–61). That can happen if the resonant terms have signs opposite to that of the sum of the nonresonant terms and, as they grow, cancel out the sum of the nonresonant terms.[7)]

[6)]An analogous assumption was made in Refs. 17 and 51 directly in the derivation of the equations for the operators $a_{\mathbf{k}}^+$, $a_{\mathbf{k}_1}^+$, and $b_{\mathbf{q}}^+$.

[7)]It should be noted that when comparing theoretical calculations with experimental results on resonance diffraction of light by sound one must, generally speaking, use a more detailed model for the light-sound interaction mechanism that would take into account, for example, the contribution to γ from exciton states in the forbidden gap, which may be considerable when $\hbar\omega_k\simeq E_g$ (Ref. 61).

As is evident from (1.46), the conduction electrons may also make a considerable contribution to the resonant scattering of light at $\hbar\omega_k \sim E_g$. The presence of conduction electrons in a degenerate semiconductor may lead to considerable change in the resonant values of the photoelasticity constants $\tilde{P}_{yxik}$ ($\tilde{P}_{yxik} = (4\pi e^2/m_0^2\omega^2\hbar^2\varepsilon_0^2)\tilde{R}_{xy}^{ik}$) provided $E_g - \hbar\omega_k$ is small enough, i.e., provided $E_g - \hbar\omega_k \lesssim (m^*/\mu)\varepsilon_F$ (here m^* is the effective mass of the conduction electrons, $\varepsilon_F = \hbar^2 p_F^2/2m^*$ is the Fermi energy of the conduction electrons, and it is assumed that $\hbar\Omega_q \ll \varepsilon_F$ and that $k, q \ll p_F$). This is due to the fact that some states in the conduction band with energies below ε_F are occupied. In addition, modulation of the conduction electron occupation numbers by the sound wave may make a significant contribution to the resonance value of γ. For the case of a degenerate semiconductor and under the same assumptions as were used in deriving Eqs. (1.51), this contribution, which is described by the second term in (1.46), will be proportional to the following expression:

$$\gamma_{el} \sim \frac{\sqrt{\varepsilon_F}}{E_g + (m^*/\mu)\,\varepsilon_F - \hbar\omega_k}, \tag{1.52}$$

where it is assumed that $\hbar\Omega_q \ll \varepsilon_F$ and that $k, q \ll p_F$.

The ratio of the contribution γ_{el} to γ from the resonance terms due to modulation of the conduction-electron occupation numbers by the sound wave to the contribution γ_{ph} from terms due to photoelasticity $\tilde{p}_{yxik}$ (with allowance for occupation of conduction-band states by electrons) for a degenerate semiconductor when $\hbar\Omega_q \lesssim (m^*/\mu)\varepsilon_F$ and $E_g - \hbar\omega_k \lesssim (m^*/\mu)\varepsilon_F$ is $\gamma_{el}/\gamma_{ph} \simeq m^*/\mu$. Thus, the two contributions may be of the same order if the light frequency is close enough to $E_g/\hbar$. For the case of a nondegenerate semiconductor with $\hbar\Omega_q < E_g - \hbar\omega_k \lesssim (m^*/\mu)T$ (T is the electron temperature in energy units) we have

$$\frac{\gamma_{el}}{\gamma_{ph}} \sim \frac{n}{N_c}\sqrt{\frac{m^*}{\mu}\frac{E_g - \hbar\omega_k}{T}},$$

where N_c is the effective density of states in the conduction band. When $n \sim N_c$ and $E_g - \hbar\omega_k \sim T$ the two contributions may be of the same order. The contribution to resonance diffraction due to the presence of an electron-density wave in the case in which the conduction electrons interact with the sound wave through the piezopotential has been discussed by Levin *et al.*,[62] who showed that this contribution may be considerable.

We note that in the calculations in this part of the paper it is assumed that the propagation vectors of the photons and phonons are well determined. Owing to the limited size of the crystal in the y direction in the geometry we are considering, however, the propagation vector of the phonons is, strictly speaking, smeared out to the extent $\Delta q_y \sim 1/d$, and there is a corresponding smearing of the angle defining the phonon propagation direction: $\Delta\varphi \sim 1/qd$. If this smearing is to be negligible for one-phonon processes, it is necessary that $\Delta\varphi \ll \theta_6$, where θ_6 is the Bragg angle of incidence of the light on the specimen, i.e., $q^2d/k\sqrt{\varepsilon_0} \gg 1$ (with $\theta_6 \ll 1$), which coincides with the conditions for Bragg diffraction when the sound waves are not too intense—when $v \lesssim 1$ (see above).

Correspondingly, when $\Delta\varphi \gg \theta_6$, θ, i.e., when $q^2d/k\sqrt{\varepsilon_0} \ll 1$ and $qd\theta/\sqrt{\varepsilon_0} \ll 1$, many comparable orders of diffraction may appear at once (the Raman-Nath case for $\theta \approx 0$).

2. EXPERIMENTAL STUDY OF ACOUSTO-OPTICAL PHENOMENA IN SOLIDS

a) Experimental techniques for investigating the diffraction of light by sound

A typical setup for observing the diffraction of coherent light by coherent sound is exhibited in Fig. 2. Plane polarized radiation from the light source LS (a laser, usually operated in the lowest TEM_{00} mode to assure minimum beam spread) is brought through a system for defining the plane of polarization (a half-wave plate $\lambda/2$ and a polarizer P_1) and falls on the crystal Cr being investigated, which is mounted on the turntable T. The turntable T carries a scale on which the angle of incidence of the beam onto the specimen can be accurately read. A traveling (or standing) acoustic wave is excited in the crystal by an electromechanical transducer Tr (consisting, for example, of a half-wave piezoelectric plate) fed by an rf oscillator. The diffracted light leaving the crystal is registered by an optical system consisting of a polarization analyzer P_2, a converging lens L, a field of view stop S, and a photodetector PhD (when working in the optical and the near infrared regions the PhD is usually a photomultiplier). The signal from the PhD is then displayed or recorded by a suitable device (an oscillograph or an x-y plotter). The entire registering system is mounted on a rotatable bench whose rotation axis coincides with that of the turntable T; provision was made for accurately measuring the angle θ_{sc} through which the optical bench was turned with respect to the direction of the undiffracted beam that passed through the crystal.

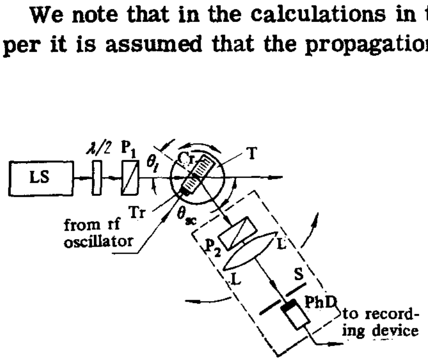

FIG. 2. Optical scheme for observing the diffraction of light by sound.

This scheme is fairly simple and makes it possible to investigate the most important characteristics of the diffraction phenomena—the spatial (angular), polarization, and amplitude characteristics. But for a complete description of the diffraction in the general case it is necessary also to know the frequency spectrum of the diffracted light. That information can be obtained with the scheme described above by mixing the incident and diffracted radiations in the photodetector (the optical heterodyne method[63,64]). In this method (Fig. 3) the heterodyne (I_H) and diffracted (I_1) beams strike the sur-

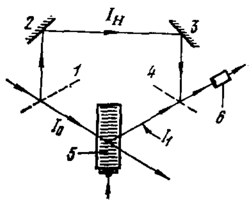

FIG. 3. Optical heterodyne scheme: I_0, I_1, and I_H—incident, diffracted, and heterodyne beams, respectively; 1, 4—half-silvered mirrors; 2, 3—opaque mirrors; 5—"ultrasound-irradiated" specimen; 6—photodetector.

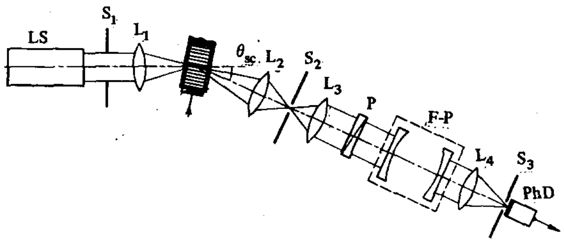

FIG. 4. Scheme for measuring the spatial and frequency spectra of diffracted light using a Fabry–Perot interferometer.

face of the fast photodetector (6) collinearly and at the output of the detector there is developed a signal at the difference (or intermediate) frequency ω_{if} (in the case of first order diffraction ω_{if} is equal to the frequency Ω of the sound) whose amplitude is proportional to the product $I_1 I_H$ of the intensities of the two beams. Then, as was shown in Ref. 64, it not only becomes possible to investigate the frequency spectrum of the diffracted light, but the sensitivity of the measurements of the intensities of the diffracted beams increases considerably (by three or four orders of magnitude as compared with the sensitivity achieved without heterodyning). If this method is to be used to study the diffraction of light by hypersound, however, extremely high frequency photodetectors will obviously have to be used.

A Fabry-Perot interferometer can also be used to study the frequency spectrum of the diffracted light.[5,7,65] Despite the relative complexity of the apparatus, this is essentially the only method available at present for investigating diffraction spectra at acoustic-wave frequencies above a few gigahertz, where it is difficult to employ the optical heterodyne method because of the lack of high-quality photodetectors having the necessary speed. Especially good results are obtained by using Fabry-Perot interferometers that can be tuned electrically (or by adjusting the pressure) with simultaneous recording of the spectra on the tape of an automatic recording instrument.[66] An optical scheme for such measurements is exhibited in Fig. 4. The light from the laser, after passing through the beam-shaping stop S_1, is focused by lens L_1 onto the specimen at a specified angle θ_i to the axis of the "sound-irradiated" crystal, and the light leaving the crystal at various angles θ_{sc} is analyzed by an optical system consisting of the converging lens L_2, the stop S_2, the collimating lens L_3, the polarization analyzer P, the tunable Fabry-Perot interferometer F-P, the converging lens L_4, the stop S_3, and the photodetector PhD. The signal from the photodetector is automatically plotted against the frequency to which the interferometer is tuned. Available tunable interferometers working in the optical range have a resolution $\Delta\omega$ of the order of 10 MHz and a scanning range of several gigahertz.

The problem of detecting very weak optical signals frequently arises in studies of diffraction. For example, the relative intensity of the first order diffracted beam in the scattering of He-Ne laser light ($\lambda = 0.63$ μm) by a longitudinal ultrasonic wave of intensity 1 mW/cm^2 propagating in quartz is $\sim 10^{-5}$, i.e., for the usual power I_0 ~ 1 mW of a continuously operating laser the power in the diffracted beam will be $\sim 10^{-8}$ W. If one also considers that the signals will frequently be even weaker and/or pulsed, it becomes obvious that one will have to resort to various electronic techniques of matched filtration to extract the signal from the noise. The methods of narrow band synchronous detection of continuous signals and pulse accumulation using a "time slot" (see, e.g., Ref. 67) have come to be the most widely used methods in the study of acousto-optical interaction. In addition, as was already mentioned above, a marked increase in sensitivity can also be achieved by using the optical heterodyne method.

It should also be noted, however, that when the acousto-optical phenomena involve the interaction of light with coherent sound introduced from outside, the scattering efficiency can be enhanced by exciting a more powerful sound wave. The great successes that have recently been achieved in the generation, conversion, and amplification of sound over the very wide frequency range from a few megahertz to some tens of gigahertz (see, e.g., Ref. 68) make it now possible, on the one hand, to obtain information on ever more subtle acousto-optical effects, and on the other hand, to construct very effective practical devices on the basis of acousto-optical principles.

b) Study of the diffraction of light by sound in dielectrics

1) *Angular dependence* (*isotropic case*). It follows from the theory of the scattering of light by sound (Sec. 1) that for dielectrics in which the acoustic waves are not too intense the diffraction pattern changes in an essential manner as the diffraction parameter Q passes from the region $Q \ll 1$ to the region $Q \gg 1$.[8)]

In the first case we have Raman-Nath diffraction, which is characterized by the presence of a series of diffracted beams of positive and negative orders, the angular separation between them being $\Delta\theta = \theta_{sc} = 2 \arcsin(\lambda/2\Lambda)$. In accordance with Eq. (1.22) the intensities $I_l \sim V_l^2$ of the diffracted beams of all orders are maximal for normal incidence of the light on the sound wave, i.e., for $\theta = 0$. As the angle of incidence increases (on the positive or negative side) the intensities of the

8)As was noted in Sec. 1, for large sound-wave amplitudes (more precisely, for large phase modulation of the transmitted wave, i.e. when $v \gtrsim 1$) the conditions on Q become $Q \ll 1/v$ and $Q \gg v$.

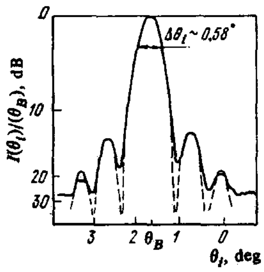

FIG. 5. Intensity of the scattered light vs angle of incidence for Bragg diffraction. The full curve represents the experimental results and the dashed curve was calculated using Eq. (2.1) for the conditions of the experiment.

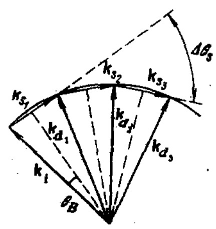

FIG. 6. Multiple successive diffraction of light by sound in the Raman-Nath regime: $\mathbf{k}_i$—propagation vector of the incident light; k_{d_j} ($j=1, 2, 3$)—propagation vector of the j-fold scattered light.

diffracted beams gradually decrease, passing through a series of successive maxima and minima. Experimental studies of the angular dependences in Raman-Nath diffraction of light have confirmed the validity of the theory.[24,69] In particular, for example, it has been shown[69] that the dependence of the number of observed diffraction peaks on the angle of incidence in the scattering of light by ultrasound in the 1–20 MHz range is in satisfactory agreement with an expression of the form of Eq. (1.22).

As has already been mentioned, diffraction for which $Q>1$ is usually called Bragg diffraction. Under the usual experimental conditions ($\lambda=0.63$ μm, $n=2$, $d\approx 1$ cm, and $v_s\approx 3\times 10^5$ cm/sec) this condition is satisfied at frequencies above ~100 MHz. According to Eq. (1.26), characteristic features of this type of diffraction are the strong dependence on the angle of incidence with the maximum diffraction efficiency at the Bragg angle, i.e., when $\sin\theta=\sin\theta_B=\mp q/2k$, and the presence under these conditions of only one first-order diffracted beam (i.e., either the beam with $l=+1$, or the beam with $l=-1$, but not both, is present). Then the angle θ_{sc} between the diffracted and transmitted beams is equal to twice the Bragg angle. According to (1.26), the angular dependence of the intensity of the diffracted light for scattering from a beam of sound waves of rectangular cross section when $v \ll 1$ has the form[9)]

$$I_1 \approx I_0 \frac{v^2}{4}\frac{\sin^2 x}{x^2}, \tag{2.1}$$

where

$$x=\frac{qd}{2}\frac{(q/2k)+\sin\theta}{\sqrt{\varepsilon_0-\sin^2\theta}}.$$

The results of an experimental study of the angular dependence of the intensity of the diffracted light ($\lambda=0.63$ μm) by an ultrasonic wave having a frequency of 800 MHz and a 2-mm wide acoustic front in a strontium titanate ($SrTiO_3$) crystal are shown in Fig. 5.[70] The curve was obtained by rotating the crystal with a fixed angle of observation equal to twice the Bragg angle. It will be seen that the intensity of the diffracted light attains its maximum value when the angle of incidence θ_i is equal to the Bragg angle θ_B, and its angular variation in accordance with (2.1) is satisfactorily described by the function $\sin^2 x/x^2$ (the dashed curve) with the argument $x=qd((q/2k)-\sin\theta)$, which agrees with the width of the cross section of the sound wave.

2) *Frequency shift of the diffracted light.* It follows from Eq. (1.14) that the frequency ω_e of the light in the diffracted beams of various orders should be shifted from the frequency of the incident light by multiples of the sound frequency Ω: $\omega_e=\omega+l\Omega$, the frequency being increased for the positive orders and decreased for the the negative ones. Physically, this is easy to explain by using Bragg diffraction as an example: negative-order diffraction results from Bragg incidence of the light onto a receding sound-wave front so, as a result of the Doppler effect, the frequency of the diffracted light should obviously be shifted toward the lower frequencies—and just by the frequency of the sound wave. It is also clear that in diffraction of positive order, which occurs when the light falls onto an approaching sound wave front, the corresponding frequency shift should be toward the higher frequencies. The frequency shifts in the higher orders for Raman-Nath diffraction can be explained in a similar manner if one takes account of the fact that they can be regarded as arising in a secondary diffraction process. Indeed, in the Raman-Nath limit we have $\theta\ll 1$, which means the the deviation angle for single scattering ($\theta_{sc}\approx 2\theta_B=\lambda/\Lambda$) is small compared with the diffraction spread of the acoustic wave ($\Delta\theta_s\approx\Lambda/d$) is small compared with the diffraction spread of the due to the finite width d of its front, i.e., $\theta_{sc}\ll\Delta\theta_s$. Then successive scattering of the light in higher orders ($\mathbf{k}_{d_1}, \mathbf{k}_{d_2}, \mathbf{k}_{d_3}, \ldots$ in Fig. 6) becomes possible, the frequency shift increasing by the frequency Ω of the sound at each step of this process.[10)]

Experimental studies using the heterodyne method, as well as studies using the Fabry-Perot interferometer,[7,65,71] have confirmed the theoretical conclusions.

[9)]Formula (2.1) serves as a particular illustration of the general proposition that the angular dependence of the amplitude of the diffracted waves of various orders when the crystal is rotated and the angle of observation is held fixed is the Fourier transform of the sound-amplitude distribution over the cross section of the beam.[29]

[10)]Generally speaking, multiple scattering is also possible in the Bragg region (e.g. from converging sound waves), but, as was noted in Ref. 9, the probabilities for such processes are not high, so in this case the higher orders would have very low intensities.

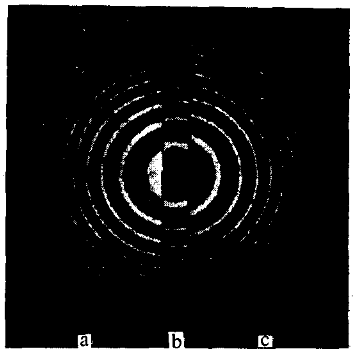

FIG. 7. Interference pattern from a Fabry–Perot etalon for diffracted (a and c) and undiffracted (b) light.

Figure 7 shows how the interference rings from a 5-cm Fabry-Perot etalon change as a result of the diffraction of light ($\lambda = 0.63$ μm) from a 790-MHz acoustic wave introduced from outside.[72] Figure 7a shows the interference rings for the case when the light is incident on a recording wave front, Fig. 7b for the case when there is no sound, and Fig. 7c for the case when the light is incident on an approaching wave front.

For the interferometer used in these experiments a shift of one ring corresponds to a frequency shift of 3 GHz. It will be seen that the frequency shift was toward the lower frequencies in case a) and toward the higher frequencies in case c), as compared with case b) in which there was no diffraction. The magnitudes of the frequency shifts obtained by comparing the shifts of the rings with the distances between them, turned out to be $\mp$790 MHz respectively for cases a) and c), i.e., the frequency shifts are very accurately equal to the frequency of the sound wave, as is to be expected when the Bragg conditions are satisfied.

It should be noted that the well verified shift observed in diffraction from sound waves now provides one of the most important bases for the design of acousto-optical data-processing devices (see Sec. 3).

3) *Amplitude characteristics.* The dependences of the intensity of the diffracted light on the amplitude Δn of the modulation of the refractive index of the matter traversed by a sound wave of rectangular cross section are given for the Raman-Nath and Bragg cases by Eqs. (1.22) and (1.26), respectively. When the angle is adjusted for maximum scattering, i.e., for normal incidence of the light beam in the first case and for incidence at the Bragg angle in the second, the corresponding dependences are as follows:

$$I_n = I_0 J_n^2(v) \qquad (n = 0, \pm 1, \pm 2, \ldots), \tag{2.2}$$

and

$$I_1 = I_0 \sin^2 \frac{v}{2}. \tag{2.3}$$

In the Raman-Nath case v is nothing other than the amplitude of the phase changes in the transmitted light. Sanders[73] measured the intensities of the light in diffracted waves of various orders as functions of v (Fig. 8). It is evident from the figure that Sanders' results for five diffraction orders are satisfactorily described by Bessel functions with the argument v (dashed curves) over a fairly wide range of v values. The discrepancy between theory and experiment at very large v values is probably due to the fact that then the conditions for pure Raman-Nath diffraction, which in this case depend on the value of v ($Q \ll 1/v$, see Subsec. b) of Sec. 1) are violated. A number of experimental studies of the amplitude dependences in both Raman-Nath and Bragg diffraction verify the validity of the available theory of the amplitude characteristics of the diffraction of light by acoustic waves in dielectrics (see, e.g., Ref. 9 and 73–75).

For the subsequent exposition we note two important features of these characteristics: first, at a definite modulation depth of the refractive index and length of the sound-wave front the entire incident power may be converted into diffracted waves of various orders (i.e., $I_0(v_{cr}) \simeq 0$), and in the Bragg region this process results in the diversion of all the incident light into the direction of a single (first-order) diffracted wave; and second, the intensity of the diffracted light in the first orders for low efficiencies is directly proportional to v^2, or, what is the same thing, to the power $P_s \sim v^2$ in the acoustic wave.

It should also be noted that all that has been said above relates to the case of the interaction of light with traveling sound waves. It is only in this case that the intensity of the light in the diffracted waves is independent of time and the frequency shift is a single valued function of the diffraction order. But, as has been shown in Refs. 6 and 76, and elsewhere, in the case of diffraction from a standing sound wave the amplitudes of the light in the diffracted waves of all orders in the general case become functions of time, whose spectrum contains even harmonics of double the sound frequency. This last is not difficult to understand since the standing wave looks to the light like a stationary diffraction grating which, however, varies with time, appearing and disappearing twice in each period of the sound wave.

4) *Diffraction in anisotropic media.* The theory of the scattering of light by sound indicates that in the general case the polarization of the diffracted light will not

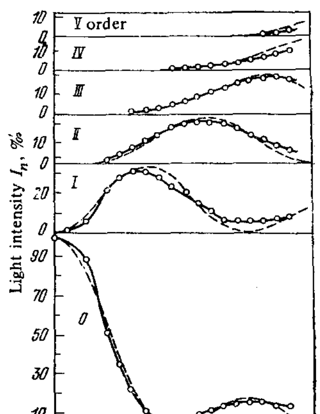

FIG. 8. Relative intensity of the light in different diffraction orders (I_n) vs the advance of the optical phase difference in the sound wave (v) for Raman-Nath diffraction in H_2O at $f_2 = 10$ MHz.

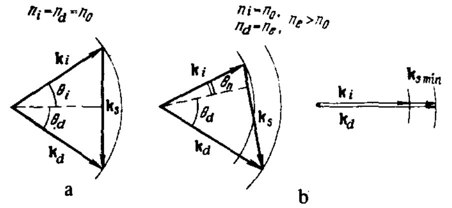

FIG. 9. Momentum conservation in acoustic scattering of light with rotation of the plane of polarization in isotropic (a) and anisotropic (b) crystals.

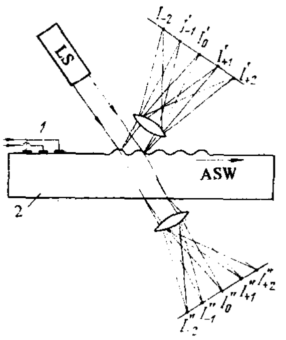

FIG. 11. Scheme for observing diffraction in transmission and in reflection with oblique incidence of light onto an elastic surface wave: 1—transducer for excitation of ASW, 2—crystal (piezoelectric, for example).

be the same as the polarization of the incident light (see Subsec. c) in Sec. 1). In particular, for example, owing to the presence of nonzero diagonal elements in the lower part of the matrix of elasto-optical coefficients of crystals,[14] transverse waves always lead to variations of the optical indicatrix in the plane of the shearing strains, and this, in turn, may lead to a change in the plane of polarization of the diffracted light.[44] In case the incident light is polarized along the principal directions of the crystal, such a rotation of the plane of polarization takes place at an angle of $\pi/2$.[15,44]

Dixon[45] showed that the conditions of synchronism for interacting waves are significantly altered in anisotropic crystals as a result of the rotation of the plane of polarization of the diffracted light. This is due to the fact that, even though the change in the energy of the light quantum on diffraction is small, the lengths of the corresponding propagation vectors differ appreciably because of the difference between the refractive indices for the incident and diffracted waves. Whereas in the case of an isotropic medium, as well as in the case of an anisotropic medium without rotation of the plane of polarization on diffraction, the strongest interaction takes place when the angles of incidence and diffraction θ_i and θ_d in the medium are equal to one another and to the Bragg angle θ_B (Fig. 9a), in the case of diffraction with rotation of the plane of polarization in an anisotropic medium (anisotropic diffraction) the angles of incidence and diffraction, in general, differ considerably from one another (Fig. 9b).

One of the important consequences of the new wave synchronism conditions is the presence of a lower bound to the frequency spectrum of the scattered phonons. As is evident from Fig. 9b, this is due to the fact that there is a minimum length $\mathbf{k}_{s\,\min}$ for the propagation vector of sound that will allow the conservation laws to be satisfied when the incident and diffracted rays have the same direction.

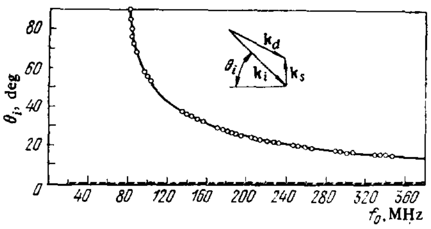

FIG. 10. Optimal angle of incidence vs sound frequency in anisotropic diffraction of light by a longitudinal ultrasonic wave propagating along the x axis in xy-cut quartz.

The modified Bragg wave synchronism law for diffraction in an anisotropic medium can be written in the form

$$\sin\theta_i = \frac{\lambda}{2v_s n_i}\left[f_s + \frac{v_s^2}{f_s\lambda^2}(n_i^2 - n_d^2)\right],$$
$$\sin\theta_d = \frac{\lambda}{2v_s n_d}\left[f_s - \frac{v_s^2}{f_s\lambda^2}(n_i^2 - n_d^2)\right], \qquad (2.4)$$

where n_i and n_d are the refractive indices of the medium for the incident and diffracted waves, respectively, and θ_i and θ_d are the corresponding angles of incidence and diffraction of the light in the medium. It follows from Eqs. (2.4) that the minimum frequency of the sound, as determined from the conditions for collinear interaction ($\theta_i = \theta_d = \pi/2$) is

$$f_{s\,\min} = \frac{v_s}{\lambda}(n_i - n_d). \qquad (2.5)$$

Thus, when the extraordinary light wave in quartz ($n_i = n_e = 1.555$) collides head on with the wave front of a longitudinal sound wave propagating in the x direction the diffracted light will be a wave with ordinary polarization ($n_d = n_0 = 1.546$). Then with $v_s = 5.75\times10^5$ cm/sec, the minimum sound frequency as given by (2.5) will be ~82 MHz. Figure 10 shows experimental data for this case on the optimal angle of incidence for most efficient light scattering as a function of the sound frequency.[45] The figure also gives the corresponding theoretical curves calculated for the usual (dashed line) and the modified (full curve) Bragg law. It will be seen that the anisotropic diffraction differs unusually strongly from the diffraction for the isotropic case and is quite well described by the modified law (2.4). Subsequent studies of acousto-optical interaction is uniaxial and biaxial crystals have confirmed the validity of Dixon's approach to the description of anisotropic diffraction and have revealed a number of otherfeatures characteristic of it.[77-79]

5) *Diffraction of light by acoustic surface waves.* A number of papers have been devoted to the experimental study of the features of the diffraction of light by acoustic surface waves (ASW).[80-87] It was found that when light is incident obliquely onto the surface of a solid on which ASW are propagating one observes diffraction in both transmitted and reflected light (Fig. 11). This is due to the fact that in addition to the photoelastic variations of the dielectric constant within the medium there are, in the general case, "ripples" (distortion of the surface

corresponding to the normal component of the ASW displacements) on the surface, and these give rise to a variable path difference for both the transmitted light waves and for the reflected ones.

Since the difference δn_r between the refractive indices in the crystal and in the air ($\delta n_r = (n_0 - 1) \sim 1$) is considerably larger than the variations δn_{ph} of the refractive index due to photoelastic effects within the wave ($\delta n_{ph} = (1/2) n_0^3 p \, \partial u/\partial x$), even when the height h_r of the "ripples" is small ($h_r \approx u_\perp$) the phase differences between various parts of the reflected-wave front due to the "ripples" ($\delta\varphi_r = K_0 \delta n_r h_r$) may become comparable with the phase difference $\delta\varphi_{ph} = K_0 \, \delta n_{ph} h_{ASW}$ due to the photoelastic variations within the crystal over a considerably longer path equal to the penetration depth of the ASW into the crystal ($h_{ASW} \sim \Lambda$, and, consequently, $\delta\varphi_{ph} \approx K_0 \delta n_{ph} \Lambda$). Taking account of the fact that $\partial u/\partial x \simeq qu$, we find that

$$\frac{\delta\varphi_r}{\delta\varphi_{ph}} \approx \frac{n_0 - 1}{\pi n_0^3} \frac{1}{p} \sim 1, \tag{2.6}$$

i.e., the ratio of the two contributions to the diffraction of light by ASW (at oblique incidence)—the "ripple" and photoelasticity contributions—is independent of both the power and the wavelength of the sound wave and is determined entirely by the optical and photoelastic properties of the medium. In Refs. 80 and 86 it has been shown, for example, that the surface distortions play a predominant role in the case of a Rayleigh wave propagating in crystalline quartz in the Y plane along the x axis.

Because the interaction length for the interaction of light with ASW is as small as it is, the Raman-Nath character of the diffraction in this case is marked and the diffraction efficiency is low (because $v \ll 1$). It should be noted, however, that this remark pertains only to the case of oblique incidence of the light onto the surface on which the ASW are propagating. It was shown in Refs. 84 and 85 that when the light propagates parallel to the surface its interaction with the surface wave takes place over a considerably longer path (of the order of the width of the wave front) and is just as effective as in the case of a bulk wave. This case of diffraction can be used for investigating the distribution of the ASW deformations in the interior of the crystal[87] and in integrated optical devices for effective acousto-optical control of light (see Sec. 3).

6) *Resonant acousto-optical interaction near the self-absorption edge.* The acousto-optical interaction in dielectrics is due to the photoelasticity of the medium, which in the general case is described by a fourth-rank tensor whose components are the elasto-optical coefficients.[14] These coefficients characterize the tendency of the material to become polarized by the action of radiation, and they may depend on the wavelength of the incident light. In particular, such behavior may be expected for wavelengths of the incident light that correspond to the width of the forbidden gap in the crystal, when the polarizability changes substantially because of interband electron transitions.[52]

The dispersion of the elasto-optical coefficients has been detected experimentally in certain cubic crystals[88] and in compounds of the A_2B_6 group.[55] In all cases the elasto-optical coefficients were found to increase with increasing frequency ω when $\hbar\omega \leq E_g$, where E_g is the width of the forbidden gap in the material.

A number of recent papers[56–61,89] have reported an extremely strong effect of resonant acousto-optical interaction at frequencies close to the self-absorption edge in piezoactive semiconducting crystals (GaAs, CdS, ZnO) in which spontaneous amplification of acoustic waves in a supersonic stream of charge carriers has been observed.[90,91] The effect manifests itself in the following behavior of the intensity of the diffracted light as a function of the frequency ω of the light; the intensity of the diffracted light has a deep narrow minimum (diffraction ceases) at a frequency somewhat lower than $E_g/\hbar$, and then the diffraction efficiency increases with increasing frequency, increasing very rapidly as the absorption edge is approached and reaching a maximum at $\hbar\omega \approx E_g$.

Figure 12 shows the characteristic form of the resonance behavior of the diffraction for the case of the scattering of light from piezoactive transverse acoustic waves in CdS which are being amplified in a direction perpendicular to the hexagonal axis of the crystal.[56] For the ordinary (and extraordinary) waves the diffraction took place with rotation of the plane of polarization by 90° and conformed to the modified Bragg law (2.4). The fact that the form of the resonance remains constant for different (including low) intensities of the acoustic flux as specified by the drift potential (curves 1 and 2 of Fig. 12) shows that the effect does not depend on any possible bending of the energy bands as a result of strong deformations produced by the sound wave. It will be seen that the effect depends neither on the frequency of the acoustic waves (curves 5 and 4) nor on the polarization of the light (curves 2 and 4). In addition, it was established that the electro-optical effect has no influence on the piezoelectric field of the wave.

The explanation of this effect given by Gelbart and Many[56] was based on Loudon's theory (see Ref. 52 and Subsec. b) of Sec. 1), in which the mechanisms of photoelasticity and their dispersion near the self-

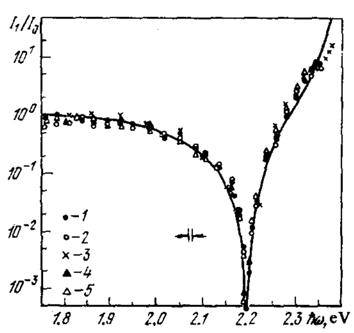

FIG. 12. Frequency dependence of the intensity of light scattered from transverse ultrasonic waves in CdS near the self absorption edge. The curve was calculated using formula (2.7). Points: 1–4—f_s = 0.8 GHz, 5—f_s = 2.5 GHz; 1—high sound intensity, 2—low sound intensity; 1–3—ordinary wave, 4–5—extraordinary wave; 3—thin (0.2 mm) specimen.

absorption edge were considered. The following approximate expression for the scattering efficiency was obtained for the experimental situation on the basis of Loudon's model:

$$\frac{I_1}{I_0'} \approx \left\{ B\left[\sqrt{E_{g\parallel}-E}\,\mathrm{arctg}\sqrt{\frac{\Delta E}{E_{g\parallel}-E}}-\sqrt{E_{g\perp}-E}\,\mathrm{arctg}\sqrt{\frac{\Delta E}{E_{g\perp}-E}}\right]-1\right\}, \tag{2.7}$$

where I_0' is the intensity of the transmitted light, $E=\hbar\omega$ is the photon energy, $E_{g\parallel}$ and $E_{g\perp}$ are the optical widths of the forbidden gap for light polarized parallel and perpendicular to the optical axis, respectively, and B is a constant that takes account of the contributions of all the matrix elements (assumed to be independent of the photon energy E). Using data[92] on the optical absorption of waves of different polarizations in CdS to evaluate $E_{g\parallel}$ and $E_{g\perp}$, treating B and ΔE as adjustable parameters and using Eq. (2.7), one can achieve good agreement between the theoretical curve (the full curve on Fig. 12) and the experimental data over a wide range of frequencies near resonance. Although the parameter values selected by the authors and the approximations used seem plausible and, qualitatively, the resonance scattering effect appears to have been correctly identified, we feel that a quantitative comparison will require further serious study of this effect.

c) Peculiarities of acousto-optical phenomena in conductive media

The presence of free electrons can substantially affect the interaction of light and sound in conducting media (see Sec. 1 above). Actually, elastic waves in any conducting media, acting through the deformation potential, will lead in principle to induced electron-density waves[93] (these are frequently called electron waves for brevity).[11)] In piezoactive semiconductors, alternating piezoelectric fields accompanying acoustic waves can also take part in the production of electron waves, and at ultrasonic frequencies this effect may become dominant and very strong.[49,95,96] In addition, as was shown in Refs. 95 and 96, the electron-phonon interaction via electrostriction may become effective in crystals having a large dielectric permittivity, and this interaction also gives rise to electron waves.

It is physically understandable that the appearance of an electron wave gives rise to an additional variation of the dielectric permittivity of the medium (of its electronic part), which is periodic in space and time and of the same spatial period (Λ) as the change in the lattice dielectric permittivity that is produced directly by the deformation in the acoustic-wave field and is responsible for the ordinary photoelasticity. It is also clear that in the general case the amplitude and phase of the electron waves will depend on the external fields and on the ratios of the sound frequency Ω to the conductivity relaxation frequency $\omega_c=4\pi\sigma/\varepsilon$ and to the diffusion frequency $\omega_D=v_s^2/D_{e1}$ (where D_{e1} is the electron diffusion coefficient).

[11)]Here, for simplicity, we discuss neither electron-temperature waves nor holes in semiconductors, which can also take part in these processes (see Sec. 1).

Thus, an acoustic wave in a conductive medium gives rise to two gratings capable of diffracting light, which have the same spatial period but different "amplitudes" and, generally speaking, are shifted in phase with respect to one another.

Such electronic diffraction gratings were first discovered[36] in n-type piezoelectric photoconductive CdS crystals, using light of 10.6 μm wavelength. The following experimental procedures have been used to distinguish between diffraction by electron waves and diffraction resulting from the elasto-optical interaction:

1) Highly photosensitive specimens were chosen so that one could obtain a low dark conductivity ($\sigma_1=10^{-7}$ $(\Omega\,\mathrm{cm})^{-1}$) as well as a fairly high conductivity ($\sigma_2=3\times10^{-3}$ $(\Omega\,\mathrm{cm})^{-1}$) after strong preliminary irradiation; the specimens also had equally low electronic absorption for a 65 MHz transverse piezoactive ultrasonic wave. Hence the intensity of the sound (and consequently the lattice diffraction) was about the same in the two cases (with $I_s\sim1$ W/cm^2), while the "electronic" diffraction was present in one case and absent in the other (see the peak at $\theta_i\sim10°$ in Fig. 13a).

2) With the chosen propagation and polarization directions for the sound and light with respect to the crystallographic axes of the specimen (see the inset near the top of Fig. 13) the diffraction resulting from the photoelasticity effect was anisotropic, while the diffraction from the electron waves was isotropic. Then the "lattice" diffraction had a maximum at the incidence angle $\theta_i=16°$, while the "electronic" diffraction had a maximum at a different angle of incidence, $\theta_i=10.5°$ (in both cases the total scattering angle was 21°, which corresponded to a grating period $\sim\Lambda=v_s/f_s$). Accordingly, in the first case the plane of polarization of the diffracted light was rotated through 90°, while in the second case it was not (see Fig. 13b). A comparison of the measured efficiencies of "photoelastic" and "electronic" diffraction at the same sound-wave intensity gives $\xi=\eta_e/$

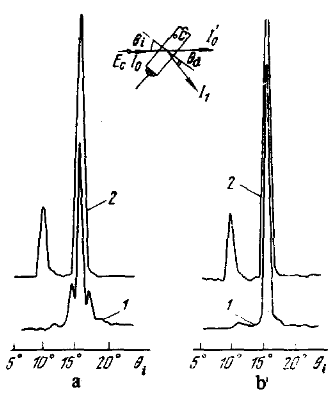

FIG. 13. Intensity of light diffracted by 65-MHz transverse piezoactive ultrasonic waves in CdS vs angle of incidence θ_i: a) for crystals of conductivity $1\times10^{-3}\,\Omega^{-1}\,\mathrm{cm}^{-1}$ (curve 1) and $3\times10^{-6}\,\Omega^{-1}\,\mathrm{cm}^{-1}$ (curve 2), the polarization plane of the scattered light being parallel to that of the incident light in both cases; (b) for the polarization plane of the scattered light perpendicular (curve 1) or parallel (curve 2) to that of the incident light, the crystal conductivity being $3\times10^{-3}\,\Omega^{-1}\,\mathrm{cm}^{-1}$ in both cases.

$\eta_{ph} \approx (1/50)-(1/100)$, and this is in satisfactory agreement with the theoretical estimate $\xi \simeq 1/100$ based on formula (1.34). It follows from formula (1.34) that in the present case the diffraction by the electron waves accompanying a piezoactive transverse wave in CdS should become predominant at wavelengths above ~30 μm for the light. The absolute efficiency of the diffraction by the "electron grating" was 5×10^{-7}. That this figure is so small is due to the fact that the experimental conditions were such that the frequency of the light was much higher than the plasma frequency of the electrons ($\omega = 1.77\times10^{14}$ sec^{-1}, while $\omega_p = \sqrt{4\pi n_0 e^2/m^*\varepsilon_0} \sim 10^{11}$ sec^{-1}), so that even if the amplitude of the density wave was relatively high ($\Delta n/n_0 \sim 1$) the modulation $\Delta\varepsilon_{el}$ of the dielectric permittivity was very small ($\Delta\varepsilon_{el} \approx (\omega_p^2/\omega^2)\Delta n/n_0 \approx 10^{-6}$), resulting in a low efficiency: $\eta_e = (\pi^2/16)(\Delta\varepsilon_{el})^2(d/\lambda)^2 \approx 5\times10^{-7}$. According to Eq. (1.34), as the frequency of the light approaches the plasma frequency under these conditions (but not conversely, since $\Delta\varepsilon_{el} = \text{const}\cdot(n_0)$ when $\Omega\tau_M \ll 1$) the electron-diffraction efficiency will increase with increasing wavelength of the radiation as λ^2. Thus, it may be supposed that diffraction due to electron waves will be as efficient in the far infrared and at submillimeter wavelengths as diffraction due to photoelasticity will be in the visible and near infrared.

d) Induced acousto-optical phenomena

In Sec. 1 we considered the induced scattering of light by sound that occurs when the sound intensity is high. Processes of this type in which thermal and acoustic vibrations take part and which are called induced Mandelstam-Brillouin scattering processes have now been studied in some detail and provide the basis for a number of interesting effects observed in the propagation of giant laser pulses through matter (see the detailed review of this topic by Starunov and Fabelinskiĭ[5]). Here we want to discuss a related process that has some special features: the induced scattering of light by coherent sound introduced from outside.

Actually, when a light beam of power P_0 is incident at the Bragg angle onto a receding (or approaching) acoustic wave (Fig. 14) the power P_1 in the diffracted beam will be given, according to Eq. (2.3) when $v \ll 1$, in terms of the sound power P_s, the parameters characterizing the material, and the geometry of the specimen by the formula

$$P_1 = \frac{\pi}{\lambda^2}\frac{d}{H} M_2 P_s P_0, \tag{2.8}$$

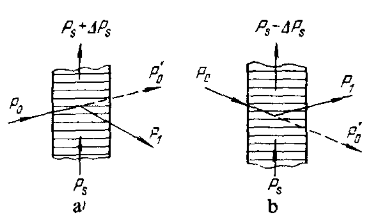

FIG. 14. Schemes for induced acousto-optical interaction with a decrease (a) or an increase (b) of the frequency of the light on scattering.

where λ is the wavelength of the light, d and H are the width and height, respectively, of the acoustic wave front, and $M_2 = n^6 p^2/\rho v_s^3$ is the acousto-optical quality factor, which contains all the relevant parameters characterizing the material.

Since Bragg diffraction is a parametric process in which a single diffracted photon arises in the course of emission or absorption of a single phonon, the power gained or lost by the acoustic wave in such a process will be

$$\Delta P_s = \frac{P_1}{\omega}\Omega, \tag{2.9}$$

where ω and Ω are the angular frequencies of the light and sound, respectively. It follows from Eqs. (2.8) and (2.9) that

$$\Delta P_s = \frac{\pi}{\lambda^2}\frac{d}{H} M_2 \frac{\Omega}{\omega} P_s P_0, \tag{2.10}$$

i.e., if the power P_0 of the incident light beam is high enough we may expect amplification or attenuation of the sound. But then if the sound power is highly amplified the diffraction of the light will also be enhanced, and this in turn will lead to a still greater amplification of the sound power and the acousto-optical interaction will become highly nonlinear.

It is evident from (2.10) that $\Delta P_s \sim P_s P_0$; hence, unlike the case of induced scattering by very weak thermal fluctuations of power P_m, in the interaction of light with a high-power external sound wave for which $P_s \gg P_m$ one can obtain amplification of the sound by light even with light fluxes of moderate power, so it will not be necessary to use giant laser pulses, which frequently lead to irreversible damage of the crystals.[5]

The amplification of coherent sound by means of induced acousto-optical interaction was first observed experimentally by Korpel *et al.*[97] In this experiment light from a pulsed ruby laser (power 1.5 kW, pulse length 0.1 μsec) was diffracted by a 45-MHz ultrasonic wave in water (diffraction efficiency $\eta \sim 10^{-4}$, i.e., $I_1 \approx 0.15$ W), and as a result the intensity of the sound was 0.06% higher at the output of the delay line than at the input. The quantity $\Delta P_s/P_s$ was estimated in accordance with (2.10) for the experimental conditions as $\sim 10^{-3}$. Subsequent experiments by a number of investigators[98–100] showed that such amplification of sound by light can be achieved in quartz, in which stable and fairly high amplification has been obtained by making use of the anisotropy of the crystal.

e) Application of acousto-optical methods to physical research

It is evident from what has been said above that the study of acousto-optical phenomena can provide valuable information both on the behavior of acoustic waves in solids under various conditions of propagation, and on the acoustic, acoustico-optical, electronic, and other properties of the solids themselves. Moreover, the acousto-optical methods of probing and diagnostics are valuable because they do not appreciably perturb the propagation of the sound.

Acousto-optical methods have long been used effectively to make acoustic waves visible, to determine the velocities, spatial periods, and shapes of the waves, their propagation direction, the intensity distributions along the propagation direction and in the cross sections, focusing characteristics, deviations of the energy flux from the direction of the wave vector, and so on (see, e.g., Refs. 29 and 101–117, as well as Bergmann's book[76]).

The use of acousto-optical methods to investigate the velocity, dispersion, and absorption of coherent sound introduced from outside as well as the corresponding properties of thermal phonons makes it possible to evaluate the elastic constants of the material with high accuracy and to investigate the mechanisms responsible for the absorption and dispersion of sound over a wide frequency range (see, e.g., Refs. 5, 7, and 118–120).

It should be especially noted that acousto-optical methods allow the characteristic mentioned above to be measured locally at a given place in the crystal rather than integrally as, for example, in the case of the well-known echo method.[121]

Acousto-optical methods are used to investigate the nonlinear effects associated with deviations from Hooke's law in the propagation of fairly intense acoustic waves in a solid (see, e.g., Refs. 122–133) and to evaluate the corresponding higher-order elastic moduli. Finally, acousto-optical measurements enable one to evaluate the photoelasticity coefficients themselves and to investigate their anisotropy (see, e.g., Refs. 134–137).

We shall not pause to discuss the papers cited above in more detail since they have already been fairly well discussed in available review articles.[118,122,125] The original method developed by Korpel[108] for the spatial amplitude-phase visualization of an acoustic image, which is based on peculiarities of the Bragg diffraction of converging light rays by sound, is an exception and we shall discuss it; it is very promising for use in nondestructive testing, medical diagnostics, acoustic holography, etc.

As an example to illustrate the possibilities of acousto-optical methods for examining the properties of solids, we present in this subsection the results of studies of certain acousto-electronic phenomena in semiconductors in which use was made of the diffraction of light by sound.

This method was first used by Zucker and Zemon[138] to investigate acoustic-noise spectra under conditions of acousto-electric (AE) current instability incident to the supersonic drift of electrons in piezoactive semiconductors.[12] By investigating the Bragg diffraction of coherent laser light by acoustic fluctuations that were being amplified along the crystal, Zucker and Zemon[138] were able comparatively simply to evaluate the acoustic-noise

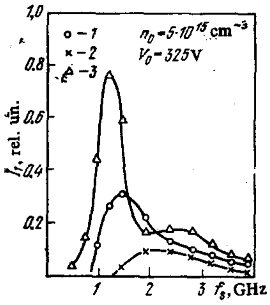

FIG. 15. Intensity of light ($\lambda_0 = 0.63\ \mu$m) diffracted by electron-drift amplified acoustic noise in n-type CdS vs frequency for several distances L from the cathode (mm): 1—0.95, 2—1.21, 3—1.47.

spectrum throughout a large solid angle and at various places in the crystal along the amplification path.

It was directly shown in a number of subsequent papers[139–142] on optical studies of AE current instability that the amplification of thermal lattice vibrations in crystals leads to moving or stationary regions of enhanced flux density—"acoustoelectric (AE) domains."

The absolute values of the integral intensity of the acoustic noise flux in AE domains as measured by diffraction[142] and acoustoelectric detection[143,144] methods agree with one another and lie in the range 10–10^4 W/cm^2, depending on the electrical conductivity. They are in satisfactory agreement with estimates based on the nonlinear theory of the amplification of acoustic waves in semiconductors.[48,49,145,146]

Optical probing of acoustic noise has led to the clarification of a number of interesting features of the amplification of such noise associated with crystal anisotropy,[141–147] with interactions of various components of the broad spectrum of fluctuations being amplified,[139–143] etc. Figure 15 shows a typical spectrum of acoustic waves in n-type CdS that are being spontaneously amplified under conditions of supersonic electron drift. It will be seen that as the distance from the front of the crystal (from the cathode) increases the frequency at the peak intensity gradually falls from its initial value of 2–3 GHz, corresponding to the frequency of maximum gain according to the linear theory, to half that value (1–1.5 GHz) in the region of fairly high sound-flux intensities.

It has been shown[148–151] that changes of that sort in the spectrum may indicate that parametric interaction of the waves being amplified play an important part in the amplification of acoustic noise. Zucker and Zemon[149] investigated the spatail variation of the amplitude of diffracted light ($\lambda = 0.63\ \mu$m) scattered in CdS by a pumping wave of frequency $\Omega_p \approx 800$ MHz and by acoustic noise with frequencies close to half the pumping frequency $\Omega_p/2 \simeq 400$ MHz in the presence of interaction between the powerful pumping wave and the noise (see Fig. 16). The figure shows that in the presence of strong pumping there is considerable increase in the noise at the frequency $\Omega_p/2$, the maximum noise increment (~22 dB/mm) considerably exceeding the drift increment of the pumping wave (~6 dB/mm). When the noise level is high enough, the power extracted by the noise from the pumping wave becomes quite considerable, and this leads to attenuation of the pumping wave.

[12] Whenever quantitative results are not required it is usually assumed that in this case the interaction of light and sound is analogous to the interaction of coherent fluxes. As was mentioned in Ref. 139, it may, generally speaking, be important to allow for the finite coherence length of the amplified noise.

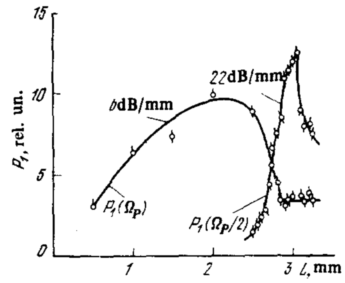

FIG. 16. Spatial variation of the power P_t of the light scattered from a transverse piezoactive ultrasonic pumping wave of frequency $\Omega_P \approx 800$ MHz $[P_t(\Omega_P)]$ and from the parametrically amplified wave $[P_t(\Omega_P/2)]$ in the electron-drift sound amplification regime in CdS.

The use of the diffraction of light by sound in the study of the acoustoelectronic interaction of two acoustic waves introduced from outside has led to very interesting results.[152] It was found, in particular, that the action of a sufficiently powerful acoustic wave could, depending on conditions, result in either a considerable increase or a considerable decrease in the electronic attenuation (or enhancement) of a second, weaker, wave.

The existence of the so-called distributed heterodyne amplification of acoustic waves in a nonlinear active medium has been established[153]; in this effect a large increment is transferred from the intermediate frequency $\Omega_i = \Omega_h \pm \Omega_s$ to the frequency Ω_s of a weakly amplified signal (Ω_h is the frequency of the heterodyne wave).

These results are in good agreement with corresponding results obtained by ordinary microwave techniques,[154–155] and also with the theory of parametric interaction of monochromatic acoustic waves in semiconductors under conditions in which sound amplification takes place.[153,156,157] The advantage of the optical method reported in Ref. 152 is that it makes it possible to trace the origin of the intermediate-frequency waves (at both the sum and the difference frequencies) as well as the spatial changes in the amplitudes of all the interacting waves, including the angular orientations of the waves with respect to one another and their distribution along the crystal.

We note, finally, that in acousto-electronic studies the acousto-optical probing method is sometimes not only convenient, but is the only method available. This is the case, for example, in the study of noise spectra (both spatial and frequency) mentioned above, the study of spatial development of nonlinear processes, the investigation of amplification in nonuniform structures,[158] and the study of acousto-electronic phenomena at very high hypersonic frequencies in the 12–100 GHz range.[159]

In concluding this subsection we list the principal characteristics of some materials that seem promising for use in acousto-optical devices (see Table I).

3. PROBLEMS OF APPLIED ACOUSTO-OPTICS

Study of acousto-optical phenomena in solids has shown that the amplitude, phase, frequency, and spatial distribution of coherently scattered light are determined by corresponding characteristics of acoustic waves. This means that it is possible in principle to control radiation by the action of sound and to use sound as an information carrying signal in optical data-processing devices. The great successes in recent years of applied research in acousto-optics have clearly shown that it is practically possible to produce a number of new acousto-optical (AO) devices for communication systems, optical memory units, projections television, signal processing, and other systems. Below we shall briefly examine some of the AO devices that have already been developed: modulators, light deviating devices (deflectors), and devices for processing signals.

a) Acousto-optical light modulators

For holographic memory units and optical communications systems, as well as in a number of other applications, it is necessary to modulate the intensity of the transmitted light in accordance with a given signal. There are two types of AO modulators that are suitable for this purpose: photoelastic modulators that make use of birefringence, and diffraction modulators.

The operating principle of the AO modulators of the first type[160,161] is similar to that of the well-known electro-optical modulators: the birefringence induced by the deformations due to a standing acoustic wave gives rise to a phase difference $\Delta\varphi$ between two differently polarized components of a light beam incident on the crystal and passing through the sound beam; this phase difference $\Delta\varphi$ is proportional to the amplitude of the deformations, and when the light is subsequently passed through a polarization analyzer, the transmitted intensity will be a function of the power in the sound wave. In the general case, the frequency spectrum of the modulation contains a constant component and even harmonics of the sound frequency, while the amplitude characteristic is nonlinear, having the form $\eta \approx \sin^2(\Delta\varphi/2)$. The modulation frequency is bounded below by the reciprocal of the time required to establish the standing wave: $f_{\min} \gtrsim 1/\tau_s = v_s/2L$, where L is the length of the crystal. When the dimensions of the optical beam are small compared with the length of the acoustic wave, the modulation characteristic becomes linear and the spectrum narrows considerably.[162] Photoelastic modulators have very narrow pass bands, since they work at the eigenfrequencies of the acoustic resonators.

Diffraction-type AO modulators are based on the spatial separation of the diffracted light and on the dependence of the light-scattering efficiency on the power of the scattering sound wave. In fact, the intensity of the light scattered in the direction of one of the diffracted beams is given in terms of the characteristics of the material, the geometry of the situation, and the power of the sound beam in the Raman-Nath and Bragg limits by Eqs. (2.2) and (2.3), respectively. The argument in these formulas, which represents the amplitude of the optical phase difference on the interaction length d, has the following form for the case of the photoelastic mechanism:

$$v = \pi\sqrt{\frac{2}{\lambda^2}\frac{d}{H}M_2P_s}, \tag{3.1}$$

TABLE I. Acoustic and acousto-optical properties of some materials.

Material	Symmetry type	ρ, g/cm^3	λ_0, μm	n	Type and propagation direction of the ultrasonic waves	v_s, 10^5 cm/sec	$\alpha_{500\ \mathrm{MHz}}$, dB/cm	Polarization and propagation direction of the light	M_1, 10^{-7} cm^2 sec/g	M_2, 10^{-18} sec^3/g	M_3, 10^{-12} cm · sec^2/g	Transparency range, μm
Fused quartz	—	2.20	0.63	1.46	L	5.96	~3	⊥	8.05	1.56	1.35	0.2–4.5
					S	3.76	~2.2	∥ or ⊥	0.963	0.46	0.256	
α-HIO_3	mm	4.63	0.63	$n_a=1.985$	L, [010]	2.89	2.5	⊥	107	83	41	0.3–1.8
				$n_b=1.960$				∥	93	80	38	
				$n_c=1.840$								
				$b>a>c$	L, [100]	3.56		∥	125	50	35	
GaP	43m	4.13	0.63	3.31	L, [110]	6.32	1.0	∥	590	44.6	935	0.6–10
					L, [100]	4.13		∥ or ⊥, [010]	137	24.1	33.1	
GaAs	43m	5.34	1.15	3.37	L, [110]	5.15	7.3	∥	925	104	179	1–11
					S, [100]	3.32	13	∥ or ⊥, [010]	155	46.3	49.3	
TeO_2	42	5.99	0.63	$n_e=2.43$	L, [100]	2.98		[001], [010]	22.9	10.6	6.8	0.35–5
				$n_e=2.27$	L, [001]	4.20	~4	[100], [010]	142	34.5	32	
					L, [101]	3.64		[010], [101]	101	33.4	27.5	
					S, [110]	0.617	~77	Circular [001]	73	793	117	
					S, [101]	2.08		[100], [010]	75	77	36	
H_2O		1	0.63	1.33	L	1.5	500	Arbitrary	4.36	160	29.1	0.2–0.9
α-HgS	32	8.1	0.63	$n_0=2.887$	L, [001]	2.45	7.1	Ordinary	1670	953	660	0.62–16
				$n_e=3.235$				Extraordinary	250	127	99	
			1.06	$n_0=2.7$	L, [001]	2.45	7.1	Ordinary		246		
$PbMoO_4$	4/m	6.95	0.63	$n_0=2.36$	L, [001]	3.75	2.5	[100], [010]	120	35.6	32	0.42–5.5
				$n_e=2.25$								
			0.49		L, [001]	3.75	2.5	[100], [010]	177	56.1	47.5	
Pb_2MoO_5	2/m	7.1	0.63	$n_x=2.169$	L	2.95	5	[001], [010]	238	123	90	0.4–5
				$n_y=2.182$								
				$n_z=2.301$								
$LiNbO_3$	3mm	4.7	0.63	$n_0=2.29$	L, [1120]	6.57	≈0.045	∥	66.5	7.0	10.1	0.4–4.5
				$n_e=2.20$								
YFe_5O_{12}	$m3m$	5.17	1.15	2.22	L, [100]	7.21	⩽0.06	⊥	3.94	0.33	0.53	1–6
α-Al_2O_3	3m	4.0	0.63	1.76	L, [001]	11.15	<0.08	∥, [11$\bar{2}$0]	7.32	0.34	0.66	0.15–6.5
$Bi_{12}GeO_{20}$	23	9.2	0.63	2.55	L, [110]	3.42		Arbitrary	29.5	9.91	8.64	0.45–5.5
				0.51 μm	S, [100]	1.77	0.62					
$Bi_{12}SiO_{20}$	23		0.63		L, [110]	3.83		Arbitrary	33.8	9.02	8.83	0.45–7.5
$Sr_{0.75}Ba_{0.25}Nb_2O_6$	4 mm		0.63	$n_0=2.31$	L, [001]		⩽1.0	Polar., [001]	26.8	38.9	48.8	0.4–6
				$n_e=2.93$	L, [100]			Polar., [100]	26.9	2.66	4.08	
$Sr_{0.5}Ba_{0.5}Nb_2O_6$	4 mm		0.63	$n_0=2.312$	L, [001]			Polar., [001]	59.3	8.62	10.8	0.4–6
				$n_e=2.273$								
As_2S_3	Amorphous	3.20	0.63	2.61	L	2.6	~42	∥	762	433	293	0.6–11.5
			1.15	2.46	L	2.6	~42	∥	619	236		
Ag_3AsS_3	32	5.49	0.63	$n_0=2.98$	L, [001]	2.65	~25	⊥	790	380	300	0.65–13.5
				$n_e=2.7$								
$Ge_{33}As_{12}Se_{55}$	Amorphous	4.0	1.06	2.55	L	2.501	~7	Arbitrary	390	246	157	1–12
$HgAsS_2$			0.63	2.7	L	2.43	⩽5.0	»	1900	1200	780	0.64–13
ADP	$\bar{4}2m$	1.0	0.63	1.58	L, [100]	6.15		∥, [010]	16.0	2.78	2.62	0.13–1.7
					S, [100]	1.83		∥ or ⊥, [001]	3.34	6.43	1.83	
KRS-5	$\bar{4}3m$	7.37	0.63	2.6	L, [100]	2.15	~8	⊥	250	210	117	0.4–30
					L, [100]			∥	167	140	78	
					L, [111]	1.96	~8	∥	1060	1050	530	
					L, [110]	2.00		∥	640	630	315	
α-S	mmm	2.07	0.63	$n_1=1.95$	L, [100]	2.7	~50	∥, [001]	460	320	169	0.5–6.6
				$n_2=2.02$				⊥	370	260	137	
				$n_3=2.22$								
Te	6 mm	6.24	10.6	$n_0=4.8$	L, [1120]	2.2	3–5	∥, [0001]	10 200	4400	4640	5–20
				$n_e=6.2$	L, [0001]	2.2		∥, [0001]	8 700	2920	4000	
Ge	$\bar{4}3m$	5.33	4.0	4.03	L, [111]	5.6	7.6	∥	6 800	540	1230	2–20
					L, [100]	3.57	2.24	∥ or ⊥	960	190	270	
			10.6	4.00	L, [111]	5.5	7.6	∥	10 200	840	1850	
$PbSTeO_4$	Amorphous		0.63	2.28	L	3.45	~8	⊥	157	506		0.52–5.5

The signs ∥ and ⊥ indicate polarization of the light parallel and perpendicular, respectively, to the propagation vector of the sound, while L and S indicate longitudinal and transverse acoustic waves, respectively.

where H and P_s are the height of and the power in the sound beam, and $M_2 = m^6 p^2/\rho v_s^3$ is the previously introduced AO quality index of the material. It is evident from Fig. 17 that in both limiting cases the intensity I_0' of the transmitted light (the zeroth order diffracted beam) vanishes at certain values of the phase shift (at $v = 2.4$ rad in the Raman-Nath case and at $v \approx \pi$ in the Bragg case). This means that if the amplitude of a sound wave of sufficient power $P_{s\,\max}$ is modulated, the depth of modulation of the transmitted light wave may reach 100%. According to Eq. (3.1) the sound power necessary for achieving 100% modulation of the light depends on the quality index M_2 and on the ratio d/H. From this it follows that if we wish to reduce the electrical power consumed by the device we must use a material having a higher quality factor M_2 and an acoustic beam of rectangular cross section that is greatly extended in the propagation direction of the light. It is also evident from Fig. 17 that in the Bragg regime all the light is deviated under these conditions into a single (first order) diffracted beam, so that the modulation depth is 100% for both the transmitted and the diffracted light. In the case of Raman-Nath diffraction, however, the modulation depth does not exceed 35% for any of the diffracted beams (see Fig. 17).

The magnitude of the factor M_2 determines the efficiency of modulators at a single frequency. Gordon[163] showed that the requirement that AO modulators have both a broad frequency band Δf_s and a high efficiency η leads to the new quality parameter $M_1 = n^7 p^2/\rho v_s$, which represents the main requirements on the properties of the materials used for such devices. Actually, the requirement that the device have a broad frequency band imposes a limitation on the time required for the sound-wave front to cross the light beam, and hence on the

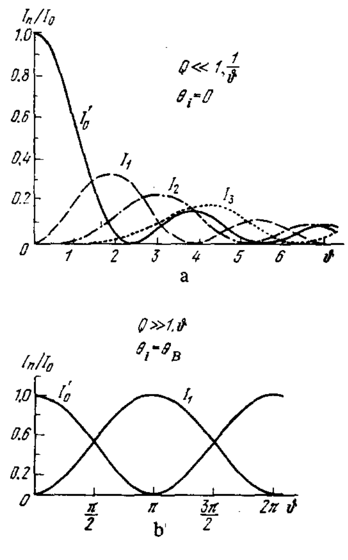

FIG. 17. Intensity of the diffracted beams of various orders in Bragg (a) and Raman-Nath (b) scattering vs the optical phase difference in the sound wave.

aperture of the beam:

$$D_{\max} = v_s \tau_{\max}. \tag{3.2}$$

If the device is to have maximum efficiency it is necessary that the optical and acoustic beams have the same angular spread, i.e., that

$$\frac{\lambda}{D_{\max}} \approx \frac{\Lambda}{d_{\max}}, \tag{3.3}$$

and this, together with Eq. (3.2) yields

$$d_{\max} \approx \frac{n}{\lambda_0} \frac{v_s^2}{f_0 \Delta f} \sim n v_s^2, \tag{3.4}$$

so that we obtain the following new quality parameter for broad band AO devices:

$$M_1 = M_2 n v_s^2 = \frac{n^7 p^2}{\rho v_s}. \tag{3.5}$$

Unfortunately, many of the material parameters can be accounted for at present only in a semiempirical manner[164] so in developing AO devices one must base the tentative designs mainly on the available experimental data (see Table I).

Analysis of the possible characteristics of AO modulators shows that when the most advantageous materials (TeO_2, As_2S_3, PbMo, Te, and others) are used these devices require less control power (under otherwise equal conditions) than the best electro-optical modulators.[165]

It should be pointed out that specific materials are chosen for AO modulators not only on the basis of the quality factor M_1 (or M_2), but also on the basis of a number of additional requirements that we have not yet discussed. Thus, for example, it must be borne in mind that in high-frequency devices the maximum aperture of the light beam is limited by the attenuation of the sound, which increases with increasing frequency; further, as the frequency increases (especially in the gigahertz range[13)]) and the relative pass band is broadened, the efficiency of the electromechanical conversion of the electrical oscillations into sound waves usually falls off considerably. In addition, requirements of optical transparency, material processing technology, etc. may be decisive in some cases.

The type M40R modulator made by Zenith Radio Corporation may serve as an example of AO modulators that have already been developed. This device makes use of longitudinal acoustic waves in chalcogenide glasses having large M_2 values and has the following characteristics[168]: $\lambda = 0.63$ μm, $\eta = 85\%$, $D = 0.65$ mm, $P_{el} = 1.6$ W (9 V into 50 Ω), $f_s = 40$ MHz, modulation depth 100% at low frequencies and 50% at 4.5 MHz, and an extinction coefficient in a diffraction order of greater than 1000. The M40R modulator can operate in the wavelength range 0.4–0.7 μm, and at $\lambda = 4.88$ μm the maximum efficiency is reached at an electrical power P_{el} of 1 W (7 V into 50 Ω).

Another way of producing effective AO light modulators is to make use of the interaction of acoustic surface waves (ASW) with light in light guides.[75,84,85,167] Under these conditions the intensity of the sound, even at relatively low ASW powers, turns out to be high enough to produce very efficient diffraction even in materials of relatively poor acousto-optical quality. In this case, however, there are additional requirements on the material: it must have good piezoelectric properties and it must be suitable for making a thin-film light guide. Good results have now been obtained by using thin ZnO films on fused quartz backings[167] and with integrated structures of specially annealed $LiNbO_3$ crystals.[75]

An integrated ASW light modulator of $LiNbO_3$ is depicted schematically in Fig. 18a. The incident radiation I_0 from a He-Ne laser is polarized along the z (x_3) axis of the crystal and is injected into the optical waveguide 2 (the hatched region) through the rutile prism 1. In the optical waveguide, which was formed on the surface of the crystal by preliminary prolonged vacuum annealing, the light beam crosses an ASW beam excited by means of the counter-stub input transducer 3. The fundamental frequency of the transducer is 78 MHz, and its pass band is ~10 MHz wide. Being diffracted by the sound, the transmitted light is broken up into a series of diffracted beams which, after leaving the device through the second rutile prism 4, can be registered in the ordinary way. Under the experimental conditions, with a beam width L of 1.2 mm, the diffraction was of intermediate type with $Q \approx 1$.

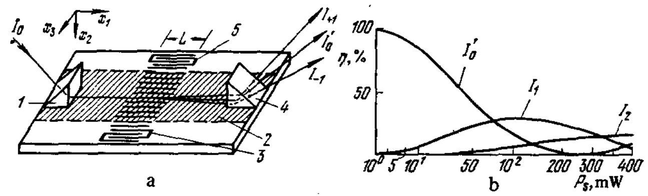

FIG. 18. Integrated acousto-optical light modulator using ASW on $LiNbO_3$. (a) Schematic drawing: 1, 4—input and output rutile prisms, 2—surface-layer light guide, 3, 5 input and output ASW transducers; b) Intensities of the diffracted beams of various orders vs the ASW power.

13) The limiting modulation frequency for such devices is always lower than the maximum frequency AB determined by the condition $f_{s\,\max} = 2v_s n/\lambda$ for collinear Bragg diffraction and usually does not exceed a few gigahertz in the visible region.

The dependences on the electrical input power of the diffraction efficiencies into the several diffracted beams (Fig. 18b) show that 100% modulation of the transmitted light is achieved at the comparatively low input power of ~250 mW. Extrapolation of these results to higher frequencies indicates, for example, that use of such structures at 180 MHz may provide an efficiency of ~70% over a pass band 43 MHz wide with an electrical power consumption of ~1.5 mW/MHz.

AO modulators can not only serve as external devices for controlling radiation from lasers, but can also take part in the process of establishing the conditions for lasing action and in the extraction of the radiation from the optical-resonator cavity. Thus, using an AO modulator employing standing acoustic waves to modulate the losses of a laser cavity at the beat frequency of the longitudinal modes leads to mode locking in pulsed lasers and to stabilization of the radiation,[168] while extraction of the diffracted radiation from resonators with opaque mirrors and continuous pumping leads to the emission of short pulses of enhanced power, the pulse separation being equal to the modulation period.[169–171] It has been reported,[170] for example, that when an He-Ne laser that could generate ~3 mW when operated continuously was equipped with an AO modulator employing 25-MHz standing acoustic waves, it generated 150-mW pulses ~0.8 nsec long at a repetition rate of 5×10^7 sec^{-1}; moreover, the electrical power required for control was only 5 mW.

As has been recently shown theoretically,[172] an acoustic wave in a laser crystal can itself assure a sufficiently strong distributed feedback and can make it possible for lasing action to take place even when there is no reflection of light from the ends. It turns out that in this case one can obtain generated light with a narrower spectrum (at least for injection lasers) and that the generated lines can be modulated in amplitude and frequency by altering the amplitude and frequency of the acoustic wave. Moreover, the lower optical loading at the ends of the crystal should reduce the rate of degradation of the end faces.

b) Light deviating devices (deflectors)

Back in 1932, Lucas and Biquard[4] showed that light waves may be highly curved in the field of a sound wave. Figure 19 shows their results on the course of the rays for a half period of the sound wave with normal incidence of the light onto the sound wave. The reduced path length of the light along the y axis, i.e., the quantity $Y=(2\pi/\Lambda_s)y\sqrt{\Delta n/n_0}$, where Δn is the amplitude of the variations of the refractive index of the medium, is plotted along the horizontal axis, and the phase φ of the sinusoidal sound wave is plotted along the vertical axis. It will be seen that the inclination of the rays in all sections $Y<\pi/2$ is a periodic function for which the rays enter the wave field at $Y=0$.[14] This means that with limited width of the traveling sound-wave front the light rays with

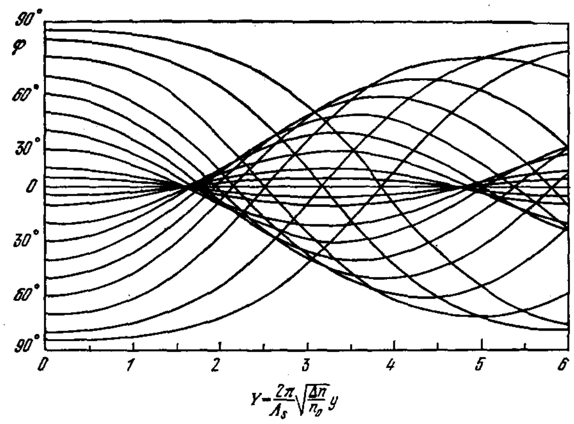

FIG. 19. Behavior of light rays in the field of an ultrasonic wave.

aperture $D<\Lambda/4$ at the entrance will be deflected periodically in time with the angular amplitude θ_{max} corresponding to the deflection of rays entering the wave at $\varphi=\pi/4$ (in the first approximation the deflection follows a sine law with the frequency f_s [173]). The number N of resolved positions at the output of such a deflector, defined as the ratio of the total deflection angle $2\theta_{max}$ to the angular (diffraction) spread $\Delta\theta$ of the beam, is limited on account of the decrease of the deflection angle at very large Y (see Fig. 19), so that

$$N_{max}=\frac{2\theta_{max}}{\Delta\theta}\approx\frac{1}{8}\frac{\Lambda^2}{\lambda d}\approx\frac{1}{Q}. \qquad (3.6)$$

It follows from Eq. (3.6) that usable resolution can be obtained with such devices only in the low-frequency region under conditions of Raman-Nath diffraction, i.e., when $Q\ll1$. In addition, it is evident from the previous discussion that the deflection angle, and therefore the resolution, of such deflectors is proportional to the acoustic power, and as a result the maximum deflection angle may be limited by the mechanical strength of the crystal (in quartz, for example, $\theta_{max}<1°$ at 145 kHz for this reason[148]).

Using two orthogonal cells of this type, Aas and Erf[176] constructed a two-coordinate deflector having a total of ~200 resolved positions.

Diffraction-type AO modulators are based on the dependence of the light scattering angle θ_{sc} on the sound frequency. Theory (see Subsec. a) of Sec. 1) shows that

$$\theta_{sc}=2\arcsin\frac{1}{2}\frac{\lambda}{\Lambda}, \qquad (3.7)$$

and

$$\Delta\theta_{sc}=\frac{\lambda}{v_s\cos(\theta_{sc}/2)}\Delta f. \qquad (3.8)$$

Taking account of the fact that we have $\Delta\theta_l\approx\lambda/D$ for the angular spread of the light beam and making use of the Rayleigh criterion, we obtain the following expression for the number of allowed positions of the beam in a diffraction type AO deflector from Eq. (3.8):

$$N=\frac{\Delta\theta_{sc}}{\Delta\theta_l}\approx\frac{D}{v_s\cos(\theta_{sc}/2)}\Delta f=\tau\Delta f, \qquad (3.9)$$

[14] More detailed information on the nature of passage of light through the field of traveling and standing waves will be found in Refs. 174 and 175.

where τ is the time lage of the device which, in the isotropic case, is the time required for the sound wave to cross the light beam.

Thus, the resolution of diffraction type deflectors increases with increasing width of the sound frequency band, and it is consequently advantageous to use high-frequency Bragg diffraction in them. In this case the change in the sound frequency should not violate the Bragg condition for interaction at all frequencies. For a fixed position of the light beam with respect to the crystal, this can be achieved, for example, provided the spread $\Delta\theta_s = \Lambda/d$ of the acoustic wave exceeds the optical beam spread $\Delta\theta_l$ and the necessary changes in the Bragg angle $\Delta\theta_B$, so that different parts of the acoustic beam take part in the diffraction at different frequencies, i.e.,

$$\Delta\theta_B(\Delta f) \leqslant \Delta\theta_s, \qquad (3.10)$$

from which it follows that for the isotropic case we have

$$\Delta f \leqslant \frac{2v_s^2}{\lambda f_s d}. \qquad (3.11)$$

It follows from (3.9) and (3.11) that in the case under consideration the requirement for high resolution limits the maximum size d of the sound wave front, i.e., it comes into conflict with the requirement that the AO device have high efficiency (see the preceding subsection). By using materials of high AO quality one can construct fairly effective deflectors of this type for sound frequencies up to ~50 MHz. Thus, for a deflector utilizing glass with the central frequency $f_0 = 40$ MHz and the frequency band $\Delta f = 20$ MHz with a beam aperture of $D = 2.5$ cm ($\tau = 6.5$ sec) and an efficiency of 60%, the maximum number of resolved beam positions turned out to be ~130.[166]

To further increase the resolution while keeping the efficiency high (or to increase the efficiency at the same resolution) Korpel *et al.*[177] proposed a method of controlling the direction of the acoustic wave while varying its frequency in such a manner that the Bragg incidence angle would be automatically preserved for all the acoustic and optical rays in a given band (Fig. 20). In this case the efficiency will be in principle independent of the frequency band since the entire acoustic beam (and not just a part of it as usual—see Fig. 20, b) will take part in scattering the light at all frequencies.

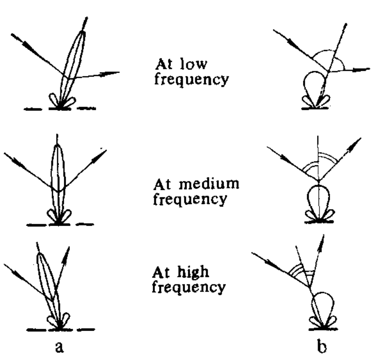

FIG. 20. Interaction of light with a controlled (a) and a fixed (b) acoustic beam in a broad-band acousto-optical device.

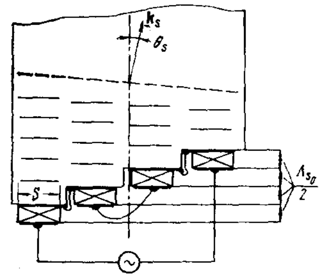
FIG. 21. A very simple acoustic diffraction grating for controlling the direction of an acoustic beam as its frequency is changed.

The simplest way to match the sound deviation angle with the change in the Bragg ray is to use an acoustic diffraction grating generated by a series of acoustic transfucers each of which is 180° out of phase with its neighbors, as shown in Fig. 21. On calculating the deflection of the sound propagation vector from the normal to the surface of the transducers as a function of frequency we obtain

$$\theta_s = \frac{\Lambda}{2s} = \frac{v_s}{2sf_s} \qquad (3.12)$$

for the case under consideration. Hence for small deflection angles (in a narrow frequency band) the condition that the deflection angle be equal to the Bragg angle ($|\Delta\theta_s| = |\Delta\theta_B|$) yields

$$\frac{v_s\Delta f}{2sf_s^2} \approx \frac{1}{2}\frac{\lambda\Delta f}{v_s} \rightarrow s = \frac{\Lambda^2}{\lambda}, \qquad (3.13)$$

where s is the width of one transducer. A rigorous calculation of the dependence $\Delta\theta_s/(\Delta f)$ for finite Δf shows that the changes $\Delta\theta_s$ and $\Delta\theta_B$ will match provided[178]

$$\Delta f \ll \frac{2v_s}{\sqrt{\lambda d}}, \qquad (3.14)$$

where $d = nS$ (n is the number of transducers generating the grating). Thus, in the final analysis, here, too, although to a lesser degree than in the preceding case, there is a conflict between resolution and efficiency. In principle, this conflict can be avoided by phasing the elements of the acoustic diffraction grating in an appropriate frequency-dependent manner[179] or by varying the refractive index electrically via the electro-optical effect.[180] It should nevertheless be noted that even in the simple case of phasing considered above the limitation on the frequency band of the deflector is substantially weakened and this makes it practical in some cases to increase the number of resolved states without lowering the efficiency.[177] Such a procedure enabled Korpel *et al.*[181] to develop a laser-beam deflector that was compatible with a projection television system; it had $N = 200$ resolved states with the acoustic frequency varying within a band of width $\Delta f = 16$ MHz. Zenith Radio Corporation developed a special glass AO deflector on this same principle which, operating at a wavelength of 0.63 μm, had $N = 400$ states per scan and a response time τ of 10 μsec at 60% efficiency.[182] The frequency dependence of the efficiency of such a deflector is shown in Fig. 22. The central frequency $f_s = 70$ MHz and the frequency band width $\Delta f = 40$ MHz correspond to scanning an optical beam with a 2×38 mm^2 rectangular aperture through an angle of 6.5×10^{-3} rad (0.375°). This is done with an

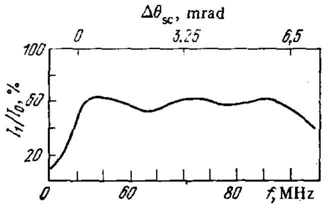

FIG. 22. Frequency characteristic of the Zenith type D70R acousto-optical deflector.

electrical power consumption of ~3.5 W (~1.3 V into 50 Ω).

Heyman and Barnard[183] have reported the construction on the basis of $PbMoO_4$, which has comparatively low acoustic losses at high frequencies, of deflectors employing phased acoustic gratings and having even higher resolution: $N=520$, $\tau=6.5$ μsec, $f_0=150$ MHz, $f=80$ MHz, $d=2.5$ cm, $D=1$ cm, and $\eta=50\%$ with $P_{el}=4$ W.

Dixon proposed a very simple way to improve the resolution of deflectors by making use of diffraction in anisotropic materials.[45] The basis for this proposal is the fact, which follows from the modified Bragg law (2.5), that, as a function of the sound frequency, the angle of incidence has a broad minimum near the acoustic frequency $f_1=(v_s/\lambda)\sqrt{n_i^2-n_d^2}$ whereas the angle of diffraction θ_d varies rapidly with the frequency (Fig. 23). This means that if the sound frequency changes within a broad band Δf near f_1 the interaction of very small changes $\Delta\theta_i$ in the angle of incidence of the light will be required to preserve synchronism, and these changes will be simply accommodated by the angular spread of the sound beam without significant reduction in the efficiency of the device. Moreover, as is evident from Fig. 23, the scanning angle of the diffracted beam corresponding to the same frequency band Δf exceeds the corresponding angle for the case of an isotropic crystal. It can be shown that the anisotropy of uniaxial crystals makes it possible to obtain an advantage in resolution given by[9]

$$\frac{N_{aniso}}{N_{iso}}\approx 2\sqrt{\frac{\Delta n_0 d}{\lambda\cos\theta_i}}\,, \tag{3.15}$$

where Δn_0 is the difference between the refractive indices for the ordinary and extraordinary rays. For some materials this advantage in resolution (or in speed) can be very great, but it is achieved only at sound frequencies f_1 in the gigahertz range. For $LiNbO_3$, for example, the increase in the frequency band width due to the anisotropy amounts to a factor of 30 at sound frequencies close to 3.6 GHz.[184]

It has been shown[185] that by putting an (isotropic) acousto-optical deflector within an optical resonator having angular degeneracy one may also obtain an increase in the number of resolved beam positions at the output of AO deflectors.

To deflect an optical beam in two coordinates one usually uses two orthogonally mounted single-coordinate deflectors such as are discussed above.[186,187] In this case one must obviously have an optical beam of circular (square) cross section, and as a result of this the height H of the acoustic beam and aperture D of the light beam in Eq. (3.1) are connected: $H=D=\tau v_s$. Then the efficiency of such devices will be characterized by a new AO quality parameter $M_3=v_s^{-1}M_1=n^1p^2/\rho v_s^2$ (see Table I).

c) Signal processing devices

Acousto-optical interactions in solids can serve as a basis for the construction of a device for the coherent processing of signals where optical spatial modulation of the signals is required. Such devices include optical devices for spatial filtration of signals in real time for computing technology,[188] devices for delaying, compressing, folding, and correlating pulsed radar signals,[189,190] optical memory systems,[191] etc. This is due in principle to the possibility of converting any signal information into a comparatively slow acoustic wave which could confine the information from a very long electromagnetic signal within a fairly short transparent crystal. The subsequent "instantaneous" reading of all the information stored in the pulse via coherent scattering of light by the pulse over its entire length thus allows one to realize parallel processing of the data, i.e., it considerably increases the transfer rate, which is an important factor in modern information systems.

The simplest acousto-optical data-processing devices (processors) that are already finding application in radar technology are dispersion type elasto-optical delay lines for linearly frequency-modulated (LFM) signals and delay lines with smoothly variable delay times.[192] These and other devices are based on optical heterodyning of diffracted light,[67] which makes it possible to extract a signal at the output of the photodetector which has the frequency, amplitude, and phase of the acoustic wave that carries information on the pulsed signal. By using a narrow optical beam to read this information in different sections along the path of the sound in the crystal one can obtain signals having different time delays, and by using a broad optical beam with an LFM pulsed signal one can secure effective time compression of the pulse. The signal becomes compressed because the scattering angles for different frequencies are directly proportional to the sound frequency so that when the frequency varies linearly along the sound pulse (Fig. 24) the diffracted rays from the entire illuminated part will enter the photodetector window together.[189] Pulse compression factors exceeding 100 have been obtained in different variants of this device (using parallel or diverging

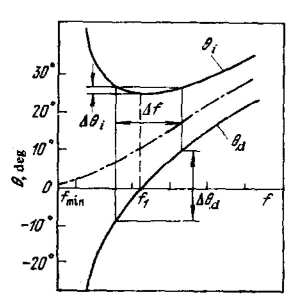

FIG. 23. Incidence and diffraction angles vs sound frequency for anisotropic diffraction.

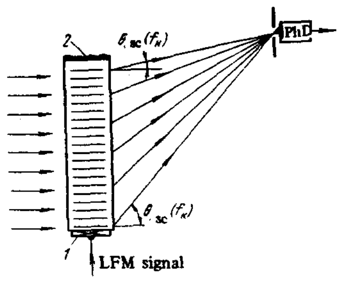

FIG. 24. Schematic diagram of an acousto-optical filter for compressing linearly frequency-modulated signals: 1—electromechanical transducer, 2—acoustic absorber.

light beams in isotropic or anisotropic media).[9,190,193–195]

A broader class of acousto-optical processors (spectrum analyzers, correlators, matched optical filters, etc.) is based on arbitrary spatial modulation of sound at the wave fronts of coherent light rays with subsequent optical processing.[91]

Figure 25a is a diagram of an acousto-optical processor based on the well known principle of spatial filtration in the Fourier plane.[196] It is clear that since $\theta_{sc}=2\theta_d$ the position of the diffraction spot on the rear focal plane of lens L will be $X^1=F(\lambda/v_s)f_s$, where F is the focal length of lens L; hence one can obtain a spectral analysis of the signal by measuring the intensity of the diffracted light as a function of the coordinate X^1. The spectral resolution, determined by the diffraction spread of the optical beam, will be $\Delta f_s=(\Delta x'/F\lambda)\,v_s=v_s/D\simeq 1/\tau_s$. This result is a consequence of the general theorem that the diffraction grating produced by the sound will effect an optical Fourier transformation of the signal. In fact, as we have already seen in Sec. 1, for the case of Bragg diffraction we can express the light field diffracted from the traveling sound wave $s(t)=s(x-v_s t)\exp[i(\Omega t-kx)]$ in the form

$$E_1 \sim E_{10}(x,\ t)\, e^{i(\omega+\Omega)t}, \tag{3.16}$$

where

$$E_{10}(x,\ t) \sim S(x-v_s t)\, e^{i(q-k)x}.$$

This gives the following result for the amplitude of the field in the diffraction spot in the focal plane of lens L [197]:

$$E(x') \sim \tilde{S}(\Omega)\, e^{i(\omega+\Omega)t}, \tag{3.17}$$

where $\tilde{S}(\Omega)=\int_{-\tau/2}^{\tau/2} S(t)e^{-i\Omega t}\,dt$ is the Fourier transform of the acoustic signal $S(t)$, and $\Omega=(2\pi/F)(v_s/\lambda)x'$. Thus, the response of a square-law photodetector with the small aperture $\Delta x'$ will be proportional to the spectral density $|d\tilde{S}(\Omega)/d\Omega|^2$ of the acoustic signal. Further, if the field $E(x')$ is mixed in the photodetector with the reference (heterodyne) field $E_H\sim E_{H_0}(x')e^{i\omega t}$ the output photocurrent will vary with time as

$$I_{\mathrm{PhC}}(t) \sim \int E^*_{H_0}(\Omega)\,\tilde{S}(\Omega)\, e^{i\omega t}\, d\Omega, \tag{3.18}$$

from which it follows that its spectrum (Fourier transform) will contain the components

$$I_{\mathrm{Ph}}(\Omega) \sim E^*_{H_0}(\Omega)\,\tilde{S}(\Omega). \tag{3.19}$$

Expression (3.19) means that in this case we have a frequency filtration of the signal $\tilde{S}(\Omega)$ with the transmission function determined by the form of the reference wave $E_{H_0}(x')$.

It can be shown that the diffraction of light by sound can also be used to effect filtration of signals in the image plane (Fig. 25b).[198] In this case the diffracted light beam is separated from the undiffracted light by a pair of confocal lenses L_1 and L_2 with a screen, so that either after L_2 (in the image plane) there is only the wave of form (3.16). After passing through the transparent filter this gives rise to the following field in the rear focal plane of lens L_3:

$$E'(t) \sim e^{i(\omega+\Omega)t}\int_{-D/2}^{D/2} S(x-v_s t)\, g(x)\, dx. \tag{3.20}$$

It is evident from this that the photodetector current will be proportional to the correlation function for the two signals $s(x)$ and $g(x)$.

The problem of using AO devices for filtration can be solved both by introducing the appropriate transparent amplitude-phase plates in the path of the diffracted light, and by forming the corresponding amplitude-phase distribution at a reference wave front. In particular, by replacing the transparent filter T in Fig. 25b by a supplementary acousto-optical modulator controlled by a second signal one can obtain the cross correlation or convolution of two signals in real time.[195,198,199]

CONCLUSION

It is difficult, in the limited space available, to give a sufficiently detailed discussion of all aspects of the present state of acousto-optics, which has seen great theoretical and experimental development in recent years. Hence our exposition of a number of questions has reduced essentially to stating known positions without giving detailed derivations or presenting finished theories. In particular, we feel that a more detailed treatment of

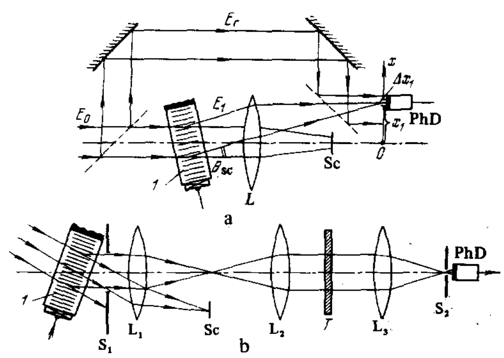

FIG. 25. Schematic diagrams of devices for the spatial processing of signals in the Fourier plane (a) and in the image plane of the acousto-optical device (b): 1—ultrasonic light modulator; L–lens, Sc—screen, S—stop, T—transparent plate, PhD—photodetector.

the mechanisms of acousto-optical interactions would be desirable when discussing the resonance phenomena near the self absorption edge where the effect of exciton states in the forbidden gap may become important, or when discussing acousto-optical phenomena in integrated optical devices where the interaction of acoustic surface waves with electromagnetic modes in thin films is very effective, etc.

The material presented in the review basically shows the results that have now been achieved in both fundamental and applied research in the field of acousto-optics. But here one can also discern a number of problems that require further theoretical and experimental study.

Despite the fact that many papers have been devoted to the development of the theory of acousto-optical phenomena we still lack a unified theory of the diffraction of electromagnetic waves by sound that would take adequate account of the properties of the material in which the diffraction takes place and would relate the magnitudes of the elasto-optical coefficients to other properties of the material (for example, to the sound velocity and absorption coefficient, etc.). Further development of the microscopic theory of photoelasticity will evidently be required before such a unified theory can be achieved, and in this connection experiments on the resonance diffraction of electromagnetic waves by sound, which will make possible a better understanding of the nature of photoelasticity, are especially interesting. The construction of such a theory would make it possible to conduct a more efficient search for new materials having low acoustic damping and large elasto-optical coefficients, which would considerably extend the range of practical applications of acousto-optics.

The experimental study of the diffraction of electromagnetic waves by sound in conducting crystals where the sound wave is accompanied by an electron-density wave is of great interest in connection with the extension of the frequency range of acousto-optical devices toward the longer wavelengths for the electromagnetic radiation (even into the submillimeter region).

Both the experimental and the theoretical study of the diffraction of electromagnetic waves by sound in thin waveguides is also of considerable interest, since in connection with the development of thin film technology it would make possible the further development of integrated acousto-optical devices.

The study of the diffraction of light by sound in active (lasing) media and, in particular, the development of the theory and the experimental study of the effect of the acoustic distributed feedback in optical masers that arises because of the modulation by the sound of both the refractive index of the medium and the absorption (or amplification) coefficient of the light may be regarded as a very interesting and promising trend in acousto-optics. It would open up the possibility of producing tunable lasers that could be tuned by means of sound, frequency modulated lasers, etc.

Of great importance for the construction of acousto-optical devices making use of powerful light beams is the study, both theoretical and experimental, of the stimulated diffraction of electromagnetic waves by coherent sound when, because of the high intensity of the light, the energy exchanged between the light and sound waves as a result of diffraction becomes so large as to alter significantly the intensity of the sound wave that does the scattering.

Finally, the search for new effective acousto-optical materials that will determine the parameters and cost of acousto-optical devices being developed remains, as before, an urgent task.

[1]L. Brillouin, Ann. Phys. (Paris) **17**, 88 (1922); Act Sci. et Ind. (Paris), fasc. 59 (1933).
[2]L. I. Mandel'shtam, Zh. Russk. fiz.-khim. o-va, ch. fiz. **58**, 381 (1926).
[3]P. Debye and F. W. Sears, Proc. Natl. Acad. Sci. USA **18**, 409 (1932).
[4]K. Lucas and P. Biquard, J. Phys. Radium **3**, 464 (1932).
[5]V. S. Starunov and I. L. Fabelinskii, Usp. Fiz. Nauk **98**, 441 (1969) [Sov. Phys. Usp. **12**, 463 (1970)].
[6]S. M. Rytov, Izv. Akad. Nauk SSSR Ser. Fiz. **2**, 223 (1937).
[7]C. F. Quate, C. D. W. Wilkinson, and D. K. Winslow, Proc. IEEE **53**, 1604 (1965).
[8]R. W. Dixon, IEEE Trans. **ED-17**, 229 (1970).
[9]W. P. Mason (editor), Physical acoustics: principles and methods, Academic Press, N. Y. 1964–75 (cited in Russ. Transl., "Mir," M., 1974, Vol. 7, p. 311).
[10]H. Y. Fan, W. Spitzer, and R. Collins, Phys. Rev. **108**, 566 (1956).
[11]A. G. Aronov, G. E. Pikus, and D. Sh. Shakhter, Fiz. Tverd. Tela (Leningrad) **10**, 822 (1968) [Sov. Phys. Solid State **10**, 645 (1968)].
[12]L. D. Landau and E. M. Lifshits, Élektrodinamika sploshnykh sred (Electrodynamics of continuous media), Gostekhizdat., M., 1957 (Engl. Transl., Pergamon Press, Oxford, N. Y., 1960).
[13]R. L. Gordon, J. Appl. Phys. **39**, 306 (1968).
[14]J. F. Nye, Physical properties of crystals, their representation by tensors and matrices, Oxford, 1957 (Russ. Transl. "Mir," M., 1967).
[15]L. L. Hope, Phys. Rev. **166**, 883 (1968).
[16]N. M. Kroll, J. Appl. Phys. **36**, 34 (1965).
[17]A. Yariv, IEEE Trans. **QE-1**, 28 (1965).
[18]G. L. Tang, J. Appl. Phys. **37**, 2945 (1966).
[19]Z. F. Krasil'nik and M. I. Rabinovich, Fiz. Tekh. Poluprovodn. **7**, 1241 (1973) [Sov. Phys. Semicond. **7**, 835 (1973)].
[20]A. B. Bhatia and W. J. Noble, Proc. R. Soc. **A220**, 356, 369 (1933).
[21]W. G. Mayer, G. B. Lamers, and D. G. Auth, J. Acoust. Soc. Am. **42**, 1255 (1967).
[22]R. J. Hallermeier and W. G. Mayer, *ibid.* **47**, 1236 (1970).
[23]G. H. Lean and G. G. Powell, Proc. IEEE **58**, 1939 (1970).
[24]C. V. Raman and N. S. Nagendra Nath, Proc. Indian Acad. Sci. **A2**, 406 (1935); **A3**, 75, 119, 459 (1936).
[25]W. R. Klein, B. D. Cook, and W. G. Mayer, Acoustica **15**, 67 (1965).
[26]W. R. Klein and B. D. Cook, IEEE Trans. **SU-14**, 123 (1967)
[27]Max Born and Emil Wolf, Principles of optics, Pergamon, N.Y., 1965 (Russ. Transl. "Nauka," M., 1970).
[28]P. Phariseau, Proc. Indian Acad. Sci. **A44**, 165 (1956).
[29]M. G. Cohen and E. I. Gordon, Bell. Syst. Techn. J. **A44**, 693 (1965).
[30]O. Leroy and R. Mertens, Proc. Indian Acad. Sci. **A68**, 296 (1968).
[31]O. Leroy, Acoustica **29**, 303 (1973); J. Sound and Vibr. **32**, 241 (1974).

[32]V. V. Proklov, G. N. Shkerdin, and Yu. V. Gulyaev, Solid State Commun. **10**, 1145 (1972).
[33]Yu. V. Gulyaev and G. N. Shkerdin, Radiotekh. Elektron. **19**, 1075 (1974).
[34]Yu. V. Gulyaev and G. N. Shkerdin, Phys. Lett. **A44**, 359 (1973).
[35]Otfried Madelung, Physics of III-V compounds, J. Wiley, N.Y., 1964 (Translated from the German; Russ. Transl. "Mir," M., 1967).
[36]Eugen Jahnke, Fritz Emde, and Friedrich Lösch, Tafeln höherer Funktionen, Teubner, Stuttgart, 1960 (Engl. Transl. of an earlier edition Dover, N.Y. 1943; Russ. Transl. "Nauka," M., 1968).
[37]V. V. Proklov, G. N. Shkerdin, and Yu. V. Gulyaev, Fiz. Tekh. Poluprovodn. **6**, 1915 (1972) [Sov. Phys. Semicond. **6**, 1646 (1972)].
[38]R. Extermann and G. Wannier, Helv. Phys. Acta **9**, 520 (1936).
[39]G. W. Willard, J. Acoust. Soc. Am. **21**, 101 (1949).
[40]F. Kuliasko, R. Mertens, and O. Leroy, Proc. Indian Acad. Sci. **A67**, 295 (1968).
[41]O. Leroy, *ibid.* **A73**, 232 (1971); Ultrasonics 181 (1972).
[42]D. L. White, J. Appl. Phys. **33**, 2547 (1962).
[43]I. L. Fabelinskiĭ, Molekulyarnoe rasseyanie sveta (Molecular scattering of light), "Nauka," M., 1965.
[44]W. T. Maloney and H. R. Carleton, IEEE Trans. **SU-14**, 135 (1967).
[45]R. W. Dixon, IEEE Trans. **QE-3**, 85 (1967).
[46]V. V. Proklov, V. I. Mirgorodskiĭ, G. N. Shkerdin, and Yu. V. Gulyaev, Pis'ma Zh. Eksp. Teor. Fiz. **19**, 13 (1974) [JETP Lett. **19**, 7 (1974)].
[47]D. F. Nelson and M. Lax, Phys. Rev. Lett. **24**, 375 (1970); Phys. Rev. **B3**, 2778 (1971).
[48]P. K. Tien, Phys. Rev. **171**, 570 (1968).
[49]Yu. V. Gulyaev, Preprint IRÉ Akad. Nauk SSSR, M., 1969; Fiz. Tverd. Tela (Leningrad) **12**, 415 (1970) [Sov. Phys. Solid State **12**, 328 (1970)]; IEE Trans. **SU-17**, 111 (1970).
[50]G. N. Shkerdin and Yu. V. Gulyaev, Fiz. Tverd. Tela (Leningrad) **16**, 3288 (1974) [Sov. Phys. Solid State **16**, 2136 (1974)].
[51]Amnon Yariv, Quantum electronics, Wiley, N.Y. 1967 (Russ. Transl. "Sov. Radio," M., 1973).
[52]R. Loudon, Proc. R. Soc. **275**, 218 (1963).
[53]P. M. Platzman and N. Tzoar, Phys. Rev. **182**, 510 (1960).
[54]A. S. Pine, *ibid.* **B5**, 3003 (1972).
[55]B. Tell, J. M. Worlock, and R. J. Martin, Appl. Phys. Lett. **6**, 129 (1965).
[56]V. Gelbart and A. Many, Phys. Lett. **A43**, 329 (1973).
[57]D. K. Garrod and R. Bray, Phys. Rev. **B6**, 1314 (1972).
[58]R. Wakita, M. Umeno, S. Hamad, and S. Miki, Jap. J. Appl. Phys. **12**, 706 (1973).
[59]V. Gelbart and A. Many, Appl. Phys. Lett. **19**, 192 (1971).
[60]R. Berkowicz and D. H. R. Price, Solid State Commun. **14**, 195 (1974).
[61]R. Berkowicz and T. Skettrup, Phys. Rev. **B11**, 2316 (1975).
[62]V. M. Levin, R. G. Maev, and Z. I. Filatova, Pis'ma Zh. Eksp. Teor. Fiz. **17**, 127 (1973) [JETP Lett. **17**, 90 (1973)].
[63]H. Z. Cummins and N. Knable, Proc. IEEE **51**, 1246 (1963).
[64]R. W. Dixon and E. I. Gordon, Bell Syst. Tech. J. **46**, 367 (1967).
[65]G. E. Fransois and A. E. Seigman, Phys. Rev. **A139**, 4 (1965).
[66]M. A. Biondi, Rev. Sci. Instrum. **27**, 36 (1956).
[67]A. M. Bonch-Bruevich, Radioélektronika v éksperimental'noĭ fizike (Electronics in experimental physics), "Nauka," M., 1966.
[68]A. I. Morozov, V. V. Proklov, B. A. Stankovskiĭ, and A. D. Gingis, P'ezopoluprovodnikovye preobrazovateli i ikh primenenie (Piezoelectric-semiconductor transducers and their application), "Énergiya," M., 1973.
[69]O. Nomoto, Kobayasi Bull. Inst. Phys. Res. **2**, 78 (1952).
[70]H. Z. Cummins, N. Knabell, L. Campbell, and Y. Yeh, Appl. Phys. Lett. **2**, 62 (1963).
[71]A. Ioshida and Y. Inuishi, Phys. Lett. **A27**, 442 (1968).
[72]A. E. Siegman, C. F. Quate, J. Bjorkholm, and G. Fransois, Appl. Phys. Lett. **5**, 1 (1964).
[73]F. H. Sanders, Can. J. Res. **A14**, 158 (1936).
[74]O. Nomoto, Proc. Phys. Math. Soc. Japan **22**, 314 (1940).
[75]R. V. Schmidt, I. P. Kaminov, and J. R. Carruthers, Appl. Phys. Lett. **23**, 417 (1973).
[76]Ludwig Bergmann, Der Ultraschall und seine Anwendung in Wissenschaft und Technik, VDI-Verlag, Berlin, 1942 (Russ. Transl. IL, M., 1957).
[77]M. S. Kharusi and C. W. Farnell, Proc. IEEE **58**, 275 (1970).
[78]V. V. Lemanov and O. V. Shakin, Pis'ma Zh. Eksp. Teor. Fiz. **13**, 549 (1971) [JETP Lett. **13**, 392 (1971)]; Fiz. Tverd. Tela (Leningrad) **14**, 229 (1972) [Sov. Phys. Solid State **14**, 184 (1972)].
[79]Yu. V. Pisarevskiĭ and I. M. Sil'vestrova, Kristallografiya **18**, 1003 (1973) [Sov. Phys. Crystallogr. **18**, 630 (1973)].
[80]E.P. Ippen, Proc. IEEE **55**, 248 (1967).
[81]D. C. Auth and W. G. Mayer, J. Appl. Phys. **38**, 5138 (1967).
[82]A. Korpel, L. J. Laub, and H. C. Sievering, Appl. Phys. Lett. **10**, 295 (1967).
[83]S. S. Karinskiĭ, V. G. Komarov, and V. D. Mondikov, Pis'ma Zh. Eksp. Teor. Fiz. **9**, 380 (1969) [JETP Lett. **9**, 225 (1969)].
[84]L. Kuhn, M. L. Dakks, P. F. Heidrich, and B. A. Scott, Appl. Phys. Lett. **17**, 265 (1970).
[85]L. Kuhn, P. F. Heidrich, and E. G. Lean, *ibid.* **19**, 428 (1971).
[86]E. Salzman and D. Weismann, J. Appl. Phys. **40**, 3408 (1969).
[87]S. V. Bogdanov and I. B. Yakovkin, Akust. Zh. **18**, 130 (1972) [Sov. Phys. Acoust. **18**, 104 (1972)].
[88]K. S. Zyengar, Nature (Lond.) **176**, 1119 (1955).
[89]M. Yamada, K. Ando, C. Hamaguchi, and J. Nakai, J. Phys. Soc. Japan **34**, 1696 (1973).
[90]A. R. Hutson, J. H. McFee, and D.L. White, Phys. Lett. **7**, 237 (1961).
[91]J. H. McFee, J. Appl. Phys. **34**, 1548 (1963).
[92]D. Dutton, Phys. Rev. **112**, 785 (1958).
[93]W. Shockley, Electrons and holes in semiconductors, Van Nostrand, 1950 (Russ. transl. presumably of this book under the title "Theory of electron-type semiconductors," IIL, M. 1963).
[94]V. L. Gurevich, Fiz. Tverd. Tela (Leningrad) **5**, 1222 (1963) [Sov. Phys. Solid State **5**, 892 (1963)].
[95]S. I. Pekar, Zh. Eksp. Teor. Fiz. **49**, 621 (1965) [Sov. Phys. JETP **22**, 431 (1966)].
[96]Yu. V. Gulyaev, Fiz. Tverd. Tela (Leningrad) **9**, 1816 (1967) [Sov. Phys. Solid State **9**, 1425 (1967)].
[97]A. Korpel, R. Adler, and B. Alpiner, Appl. Phys. Lett. **5**, 86 (1964).
[98]G. Cachier, C. R. Acad. Sci. (Paris) **B265**, 1442 (1967).
[99]M. Piltch and E. S. Cassedy, Appl. Phys. Lett. **17**, 87 (1970).
[100]Microwaves **10** (5), 12 (1971).
[101]M. Toepler, Ann. Phys. (Leipz.) **27**, 1043 (1908).
[102]E. Hiedemann and K. Osterchammel, Z. Phys. **107**, 273 (1937).
[103]E. Hiedemann, H. R. Asbach, and K. H. Hoesch, *ibid.* **90**, 332 (1934).
[104]A. Korpel, L. W. Kessler, and M. Ahmed, J. Acoust. Soc. Am. **51**, 1582 (1972).
[105]L. D. Rozenberg, Akust. Zh. **1**, 99 (1955) [Sov. Phys. Acoust. **1**, 105 (1955)].
[106]A. Korpel, Appl. Phys. Lett. **9**, 425 (1966); IEEE Spectrum **5** (10), 45 (1968); J. Acoust. Soc. Am. **49**, 1059 (1971).
[107]R. A. Smith, G. Wade, J. Powers, and C. J. Landry, J. Acoust. Soc. Am. **49**, 1062 (1971).
[108]A. Korpel, Int. J. Nondestr. Testing **1**, 337 (1970).

[109]L. W. Kessler, IEEE Trans. SU-19, 425 (1972).
[110]M. G. Cohen and E. I. Gordon, J. Appl. Phys. 38, 2340 (1967).
[111]M. G. Cohen, *ibid*. p. 3821.
[112]L. G. Merkulov and L. A. Yakovlev, Akust. Zh. 8, 99 (1962) [Sov. Phys. Acoust. 8 (1962)].
[113]K. N. Kozlovskiĭ, A. V. Ananskikh, and A. P. Lavut, Vopr. radioélektron. ser. obshchetekhn. No. 10, 70 (1968).
[114]A. J. Slobodnik, P. H. Carr, and A. J. Budrean, J. Appl. Phys. 41, 4380 (1970).
[115]A. I. Morozov, M. A. Zemlyanitsyn, and V. I. Anisimkin, Phys. Status Solidi A14, 339 (1972).
[116]R. M. White and F. W. Voltmer, Appl. Phys. Lett. 8, 40 (1966).
[117]Microwave Acoustic Handbook, Vol. 1A, Surface Wave Velocities (A. J. Slobodnik, E. D. Conway, and R. T. Delmonico, editors), L. G. Hanscom Field, Bedford, Mass., 1973, p. 77.
[118]C. D. W. Wilkinson and D. E. Caddes, J. Acoust. Soc. Am. 40, 498 (1966).
[119]D. H. McMahon, IEEE Trans. SU-14, 103 (1967).
[120]R. Vacher, J. Sapriel, and M. Boissier, J. Appl. Phys. 45, 2855 (1974).
[121]S. Eros and I. R. Reitz, *ibid*. 6, 83 (1958).
[122]L. K. Zarembo and V. A. Krasil'nikov, Vvedenie v nelineĭnuyu akustiku (Introduction to nonlinear acoustics), "Nauka," M., 1966.
[123]K. Brugger, J. Appl. Phys. 36, 759 (1965).
[124]B. A. Richardson, R. B. Tompson, and C. D. W. Wilkinson, J. Acoust. Soc. Am. 44, 1608 (1968).
[125]L. E. Hargrove and K. Achyuthan, in Physical Acoustics, Vol. II, Part B (W. P. Mason, editor), Academic Press, N. Y., London, 1965, p. 333; (cited as Russ. Transl., "Mir," M., 1969, p. 378).
[126]I. G. Mikhailov and V. A. Shutilov, Akust. Zh. 3, 203 (1957); 4, 174 (1958) [Sov. Phys. Acoust. 3, 217 (1957); 4, 174 (1958)].
[127]D. T. Blackstock, J. Acoust. Soc. Am. 39, 411 (1966).
[128]O. V. Shakin and V. V. Lemanov, Fiz. Tverd. Tela (Leningrad) 14, 1384 (1972) [Sov. Phys. Solid State 14, 1189 (1972)].
[129]A. Alippi, A. Palma, L. Palmieri, and G. Socino, J. Phys. (Paris) 33, (11), 263 (1972).
[130]J. Melngailis, A. A. Maradudin, and A. Seeger, Phys. Rev. 131, 1972 (1963).
[131]B. L. Timan and B. I. Minkov, in Materialy seminara po akustooptike (Materials from the seminar on acousto-optics), Novosibirsk, IFP SO Akad. Nauk SSSR, 1969, p. 17.
[132]P. O. Lopen, J. Appl. Phys. 39, 5400 (1968).
[133]D. H. McMahon, J. Acoust. Soc. Am. 44, 1007 (1968).
[134]D. E. Caddes and C. D. Wilkinson, IEEE J. QE-2, 330 (1966).
[135]V. V. Lemanov, O. V. Shakin, and G. A. Smolenskiĭ, Fiz. Tverd. Tela (Leningrad) 13, 533 (1971) [Sov. Phys. Solid State 13, 426 (1971)].
[136]T. M. Smith and A. Korpel, IEEE J. QE-1, 283 (1965).
[137]R. W. Dixon and M. G. Cohen, Appl. Phys. Lett. 8, 205 (1966).
[138]J. Zucker and S. Zemon, *ibid*. 9, 398 (1966); 10, 212 (1967).
[139]B. W. Hakki and R. W. Dixon, *ibid*. 14, 185 (1969).
[140]W. Wettling and M. Brunn, Phys. Lett. A27, 123 (1968).
[141]D. L. Spears and R. Bray, J. Appl. Phys. 39, 5093 (1968).
[142]K. Wakita, M. Umeno, S. Hamada, and S. Miki, Jap. J. Appl. Phys. 12, 706 (1973).
[143]S. G. Kalashnikov, V. V. Proklov, and A. I. Morozov, Fiz. Tekh. Poluprovodn. 2, 961 (1968) [Sov. Phys. Semicond. 2, 798 (1969).
[144]V. V. Proklov, Yu. V. Gulyaev, and A. I. Morozov, Fiz. Tverd. Tela (Leningrad) 14, 968 (1972) [Sov. Phys. Solid State 14, 832 (1972)].
[145]V. L. Gurevich, Fiz. Tekh. Poluprovodn. 2, 1557 (1968) [Sov. Phys. Semicond. 2, 1299 (1969)].
[146]P. N. Butcher, J. Phys. C4, 36 (1971).
[147]V. I. Pustovoĭ and L. A. Chernozatonskiĭ, Zh. Eksp. Teor. Fiz. 55, 2213 (1968) [Sov. Phys. JETP 28, 1174 (1969)]; Fiz. Tekh. Poluprovodn. 6, 1311 (1972) [Sov. Phys. Semicond. 6, 1147 (1972)].
[148]M. Schultz and B. K. Ridley, Phys. Lett. A29, 17 (1969).
[149]J. Zucker and S. Zemon, J. Acoust. Soc. Am. 49, 1037 (1971).
[150]A. M. D'yakonov and Yu. V. Ilisavskiĭ, Izv. Akad. Nauk SSSR, Ser. Fiz. 35, 907 (1967).
[151]A. M. D'yakonov, Yu. V. Ilisavskiĭ, and L. A. Kulakova, Fiz. Tverd. Tela (Leningrad) 14, 2612 (1972) [Sov. Phys. Solid State 14, 2259 (1973)].
[152]V. V. Proklov, V. I. Mirgorodskiĭ, S. V. Peshin, and B. K. Khabibullaev, in Tezisy VIII Vsesoyuznoĭ konferentsiĭ po kvantovoĭ akustike (Abstracts from the eighth All-Union conference on quantum acoustics), Kazan', 1974, p. 27.
[153]Yu. V. Gulyaev and P. E. Zil'berman, Pis'ma Zh. Eksp. Teor. Fiz. 11, 421 (1970) [JETP Lett. 11, 286 (1970)]; Fiz. Tekh. Poluprovodn. 5, 126 (1971) [Sov. Phys. Semicond. 5, 103 (1971)].
[154]V. K. Komar' and B. L. Timan, Fiz. Tverd. Tela (Leningrad) 11, 2617 (1969); 12, 304 (1970) [Sov. Phys. Solid State 11, 2110 (1970); 12, 248 (1970)].
[155]A. M. Kmita, I. M. Kotelyanskiĭ, A. V. Medved', and V. N. Fedorets, Pis'ma Zh. Eksp. Teor. Fiz. 20, 453 (1974) [JETP Lett. 20, 206 (1974)].
[156]Yu. V. Gulyaev and P. E. Siberman, Phys. Lett. A30, 378 (1969).
[157]Yu. V. Gulyaev and P. E. Sil'berman, Fiz. Tekh. Poluprovodn. 5, 126 (1971) [Sov. Phys. Semicond. 5, 103 (1971)].
[158]V. V. Proklov and B. K. Khabibullaev, in Proceedings of the Tenth International Conference on Ultrasonics, Prague, 1972, p. 160.
[159]D. G. Carlson, A. Seegmuller, E. Mosekilde, H. Cole, and J. A. Armstrong, Appl. Phys. Lett. 18, 330 (1971).
[160]I. I. Andrianova, Opt. Spektrosk. 12, 99 (1962); 14, 137 (1963) [Opt. Spectrosc. (USSR) 12, 48 (1962); 14, 70 (1963)].
[161]E. R. Mustel' and V. N. Parygin, Metody modulyatsiĭ i skanirovaniya sveta (Methods of modulating and scanning light), "Nauka," M., 1970, p. 191.
[162]M. Billardon and J. Badoz, C. R. Acad. Sci. (Paris), 262, 1672 (1966).
[163]E. I. Gordon, IEEE J. Quantum Electronics QE-2, 104 (1966).
[164]D. A. Pinnow, IEEE J. Quantum Electronics QE-6, 223 (1970).
[165]M. I. Zusman, N. K. Maneshin, and E. R. Mustel', Radiotekh. Elektron. 18, 1203 (1974).
[166]M-40R Acoustooptic Light Modulator, Zenith Radio Corp., Sept., 1970.
[167]N. Chubachi, J. Kushibiki, H. Sasaki, and Y. Kikuchi, J. Jap. Soc. Appl. Phys. 43 (Suppl.), 199 (1974).
[168]B. D. Cook and E. A. Hiedemann, J. Acoust. Soc. Am. 33, 945 (1961).
[169]D. Mayden, J. Appl. Phys. 41, 1552 (1970).
[170]J. Sapriel, Deflecteur acoustcoptique fonctionant en regime d'impulsions, Doc. de Travail EST/DEF 1548, C.N.E.T.
[171]M. Feldmann and J. Henaff, L'Onde Electrique 51, 805 (1971).
[172]Yu. V. Gulyaev and G. N. Shkerdin, Fiz. Tekh. Poluprovodn. 9, 1434 (1975) [Sov. Phys. Semicond. 9, 951 (1975)].
[173]J. Kolb and J. P. Loeber, J. Acoust. Soc. Am. 26, 249 (1954).
[174]A. J. Giarola and J. R. Billister, Proc. IEEE 51, 1150 (1963).
[175]V. A. Shutilov, Akust. Zh. 12, 239 (1966) [Sov. Phys. Acoust. 12, 205 (1966)].
[176]H. G. Aas and R. K. Erf, J. Acoust. Soc. Am. 36, 1906 (1964).
[177]A. Korpel, R. Adler, F. Desmares, and T. M. Smith, IEEE J. Quantum Electronics QE-1, 60 (1965).

[178]E. I. Gordon, Proc. IEEE **34**, 1391 (1966).
[179]G. A. Coquin, J. P. Griffin, and L. K. Anderson, IEEE Trans. SU-**17**, 34 (1970).
[180]V. I. Balakshiĭ and V. N. Parygin, Radiotekh. Elektron. **28**, 115 (1973).
[181]A. Korpel, R. Adler, P. Despares, and W. Watson, Proc. IEEE **54**, 1429 (1966).
[182]Zenith-D-70R Acoustooptic Laser deflector, Zenith Radio Corp., Sept. 1970.
[183]H. A. Heynan and G. M. Barnard, in Proceedings of the Electrooptics System-Design Conference, Plenum, N.Y., 1970, p. 640.
[184]E. G. Lean, C. F. Quate, and H. J. Shaw, Appl. Phys. Lett. **10**, 48 (1967).
[185]E. G. Lean, M. L. Dakss, and G. G. Powell, IBM J. Res. Dev. **13**, 184 (1969).
[186]D. A. Pinnow, A. G. Van Uitert, A. W. Warner, and W. A. Bonner, Appl. Phys. Lett. **15**, 83 (1969).
[187]J. Sapriel, *ibid.* **19**, 533 (1971).
[188]Kendall Preston Jr., Coherent optical computers, McGraw, 1972; (Russ. Transl. "Mir," 1974).
[189]J. S. Gerig and H. Montague, Proc. IEEE **52**, 1753 (1964).
[190]M. Arm, L. Lambert, and I. Weissman, Proc. IEEE **52**, 842 (1964).
[191]S. H. Rowe, Opt. Commun. **4**, 88 (1971).
[192]Brinza, Zarub. radioelektron. (Foreign Radioelectronics) No. 5, 22 (1970).
[193]H. R. Carleton, W. T. Maloney, and G. Meltz, Proc. IEEE **57**, 769 (1969).
[194]J. H. Collins, E. G. Lean, and H. J. Shaw, Appl. Phys. Lett. **11**, 240 (1967).
[195]V. D. Svet, Opticheskie metody obrabotki signalov (Optical signal-processing methods), "Energiya," M., 1971.
[196]George W. Stroke, Introduction to coherent optics and holography, Academic Press, 1969 (Russ. Transl. "Mir," M., 1967).
[197]L. J. Katrona, E. W. Leith, C. J. Palermo, and L. J. Porcello, IRE Trans. **IT-6**, 386 (1960).
[198]A. Korpel, Appl. Solid State Sci. **3**, 72 (1972).
[199]Dzhernigan, Tr. IIÉR **56** (3), 143 (1968).

Translated by E. Brunner